Computational methods for nano-mechanical sensors

S. Adhikari[1]

[1]Chair of Aerospace Engineering, College of Engineering, Swansea University, Singleton Park, Swansea SA2 8PP, UK

3rd International Conference on Innovations in Automation and Mechatronics Engineering - ICIAME2016, Gujarat, India

Swansea University
Prifysgol Abertawe

ZCCE

Swansea University

Swansea University

My research interests

- *Development* of fundamental computational methods for structural dynamics and uncertainty quantification
  A. Dynamics of complex systems
  B. Inverse problems for linear and non-linear dynamics
  C. Uncertainty quantification in computational mechanics
- *Applications* of computational mechanics to emerging multidisciplinary research areas
  D. Vibration energy harvesting / dynamics of wind turbines
  E. Computational nanomechanics

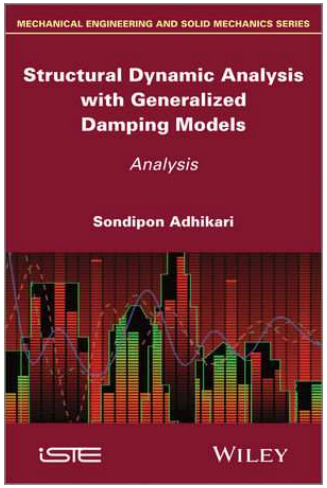

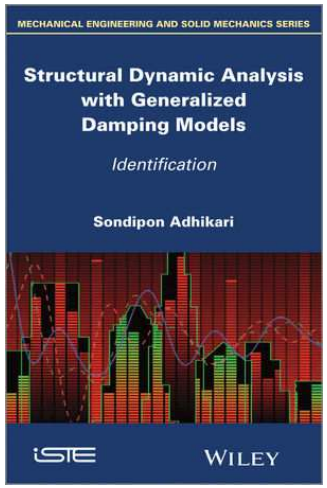

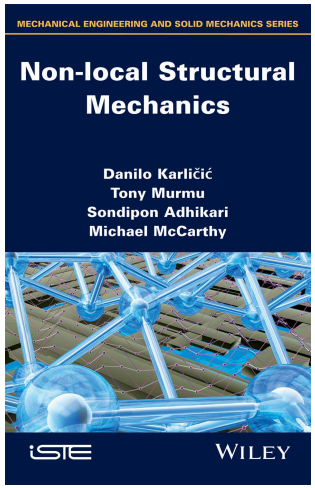

Outline

Nanoscale systems

- Nanoscale systems have length-scale in the order of $\mathcal{O}(10^{-9})$m.
- Nanoscale systems, such as those fabricated from simple and complex nanorods, nanobeams and nanoplates have attracted keen interest among scientists and engineers.
- Examples of one-dimensional nanoscale objects include (nanorod and nanobeam) carbon nanotubes (Ijima, 1993), zinc oxide (ZnO) nanowires and boron nitride (BN) nanotubes, while two-dimensional nanoscale objects include graphene sheets and BN nanosheets.
- These nanostructures are found to have exciting mechanical, chemical, electrical, optical and electronic properties.
- Nanostructures are being used in the field of nanoelectronics, nanodevices, nanosensors, nano-oscillators, nano-actuators, nanobearings, and micromechanical resonators, transporter of drugs, hydrogen storage, electrical batteries, solar cells, nanocomposites and nanooptomechanical systems (NOMS).
- Understanding the dynamics of nanostructures is crucial for the development of future generation applications in these areas.

Nanoscale systems

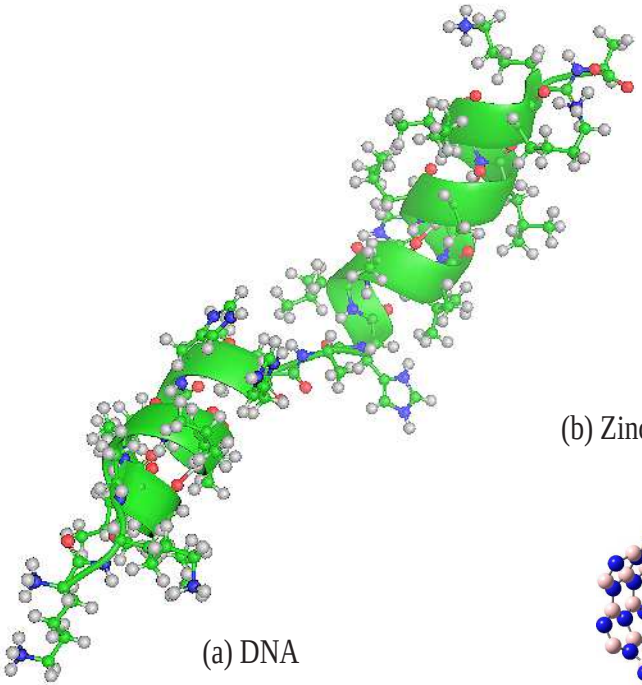

(a) DNA

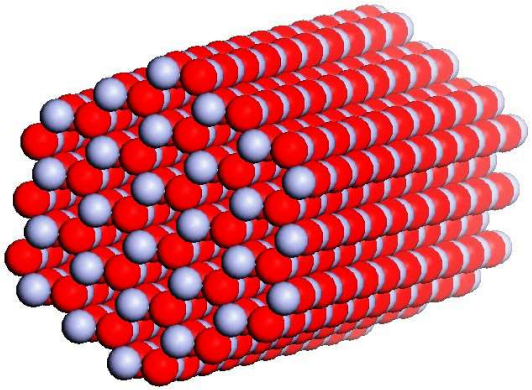

(b) Zinc Oxide (ZnO) nanowire

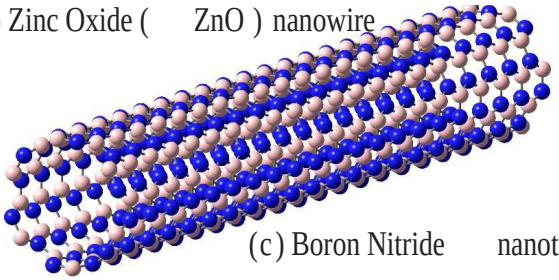

(c) Boron Nitride nanotube (BNNT)

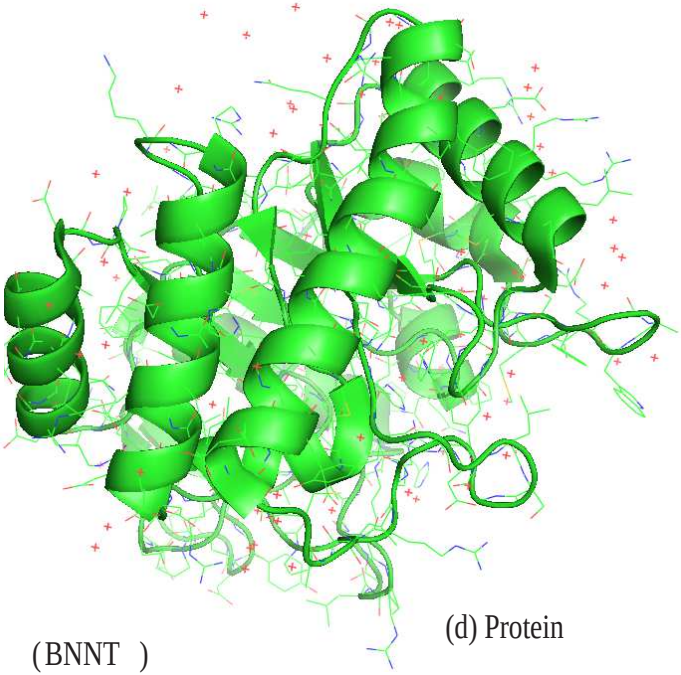

(d) Protein

General approaches for studying nanostructures

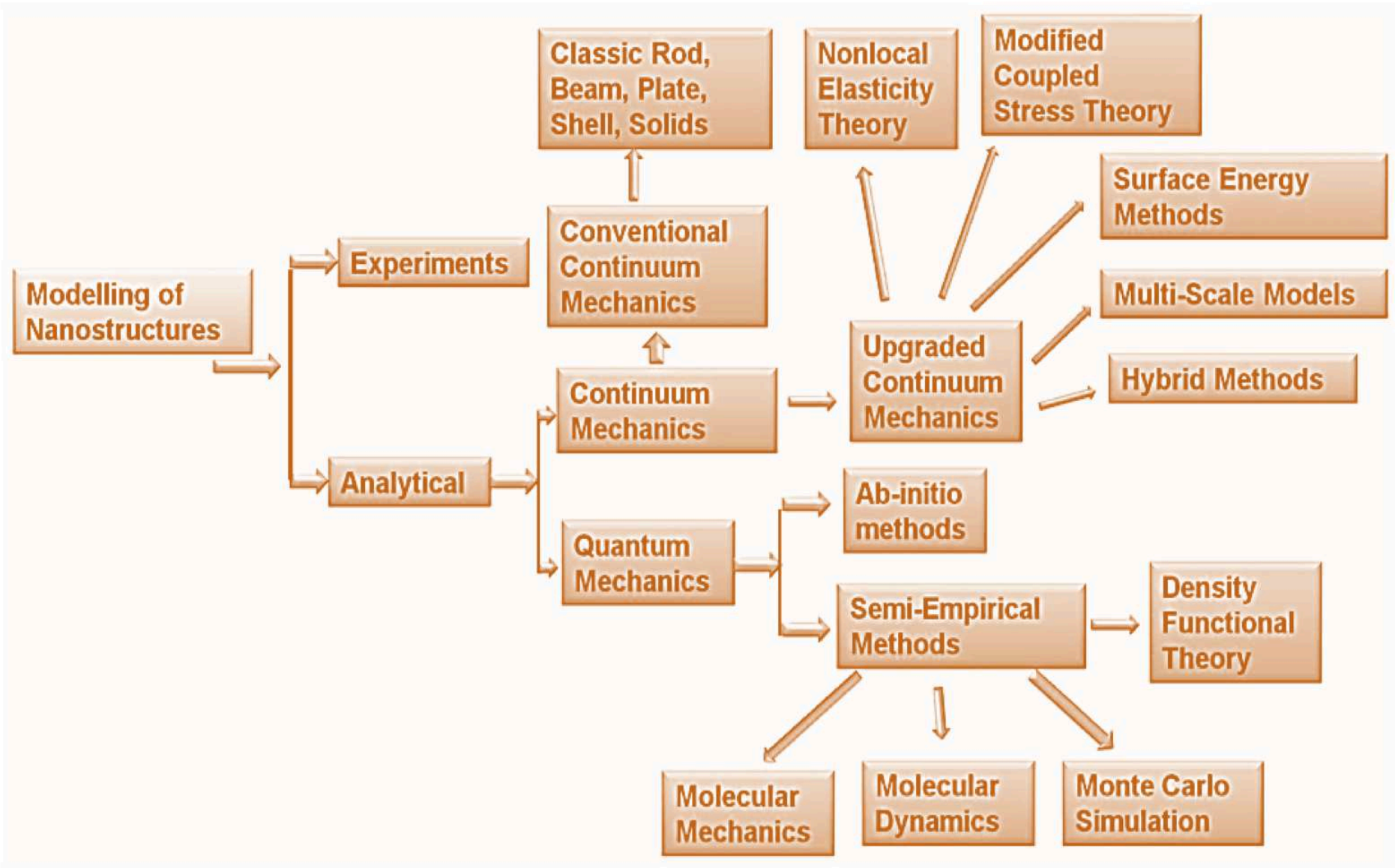

Nano mechanical sensors

- Progress in nanotechnologies has brought about a number of highly sensitive label-free biosensors.
- These include electronic biosensors based on nanowires and nanotubes, optical biosensors based on nanoparticles and mechanical biosensors based on resonant micro- and nanomechanical suspended structures.
- In these devices, molecular receptors such as antibodies or short DNA molecules are immobilized on the surface of the micro-nanostructures. The operation principle is that molecular recognition between the targeted molecules present in a sample solution and the sensor-anchored receptors gives rise to a change of the optical, electrical or mechanical properties depending on the class of sensor used.
- These sensors can be arranged in dense arrays by using established micro- and nanofabrication tools.

Cantilever nano-sensor

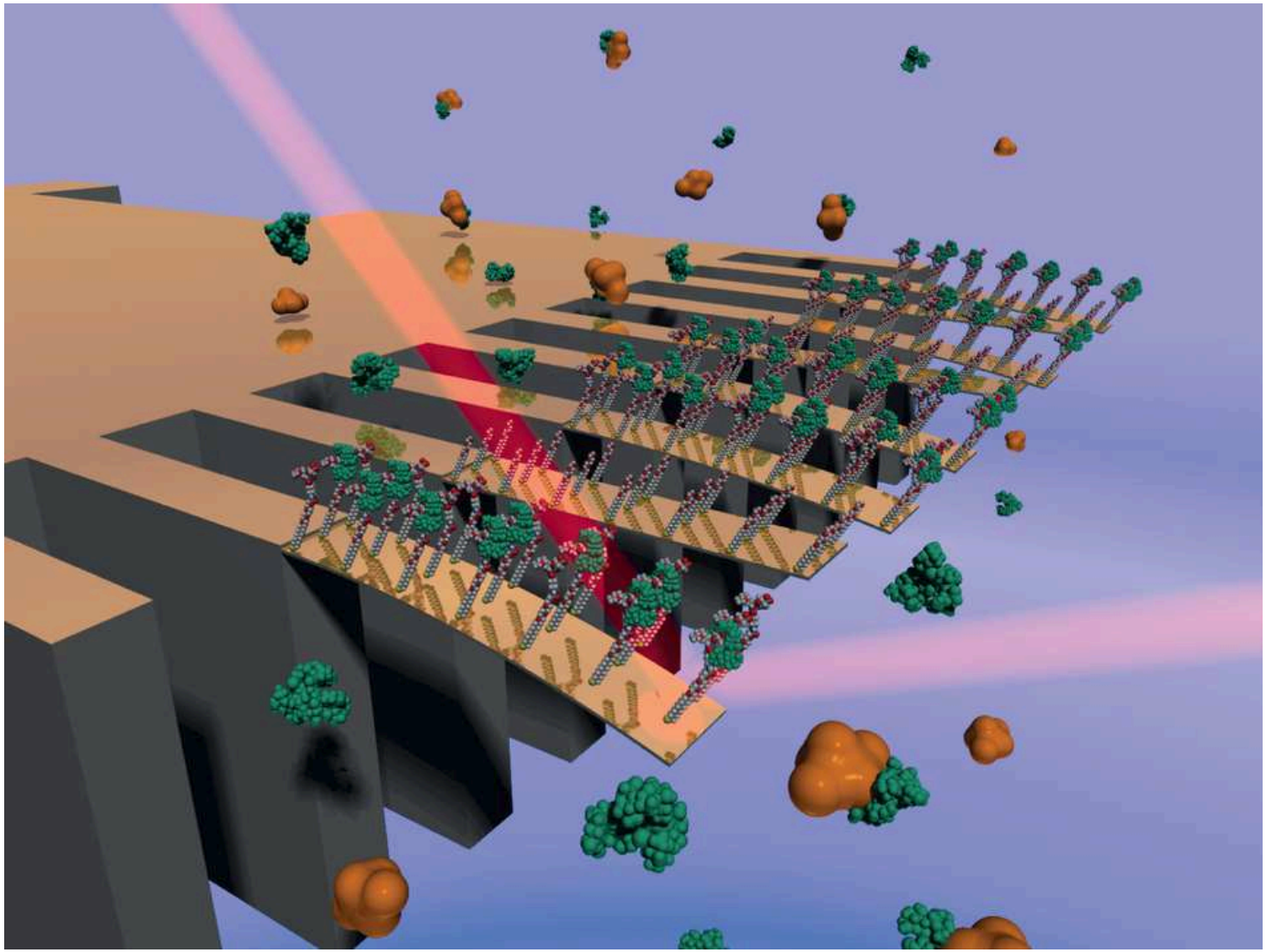

Array of cantilever nano sensors (from http://www.bio-nano-consulting.com)

Cantilever nano-sensor

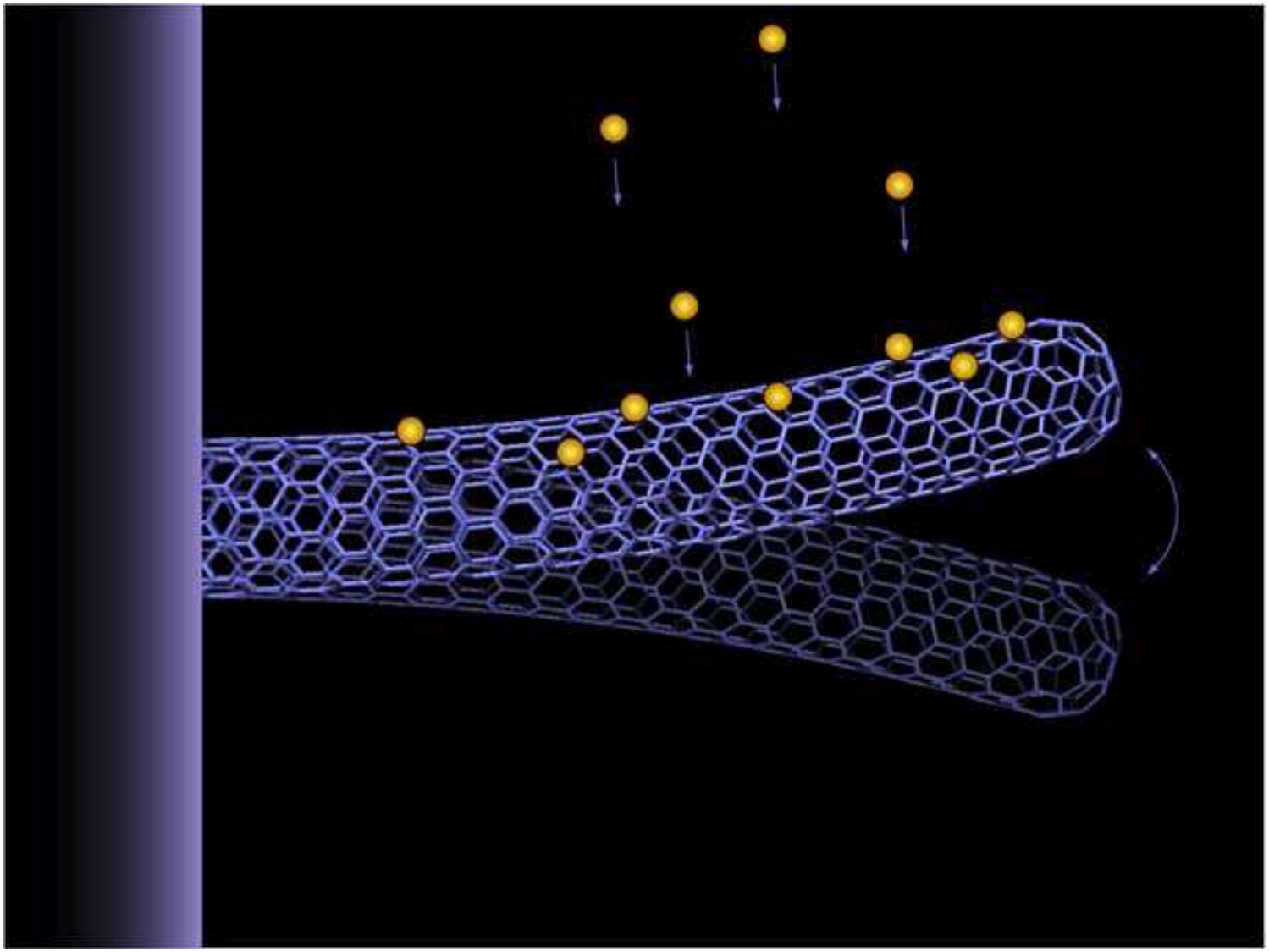

Carbon nanotube with attached molecules

The mechanics behind nano-sensors

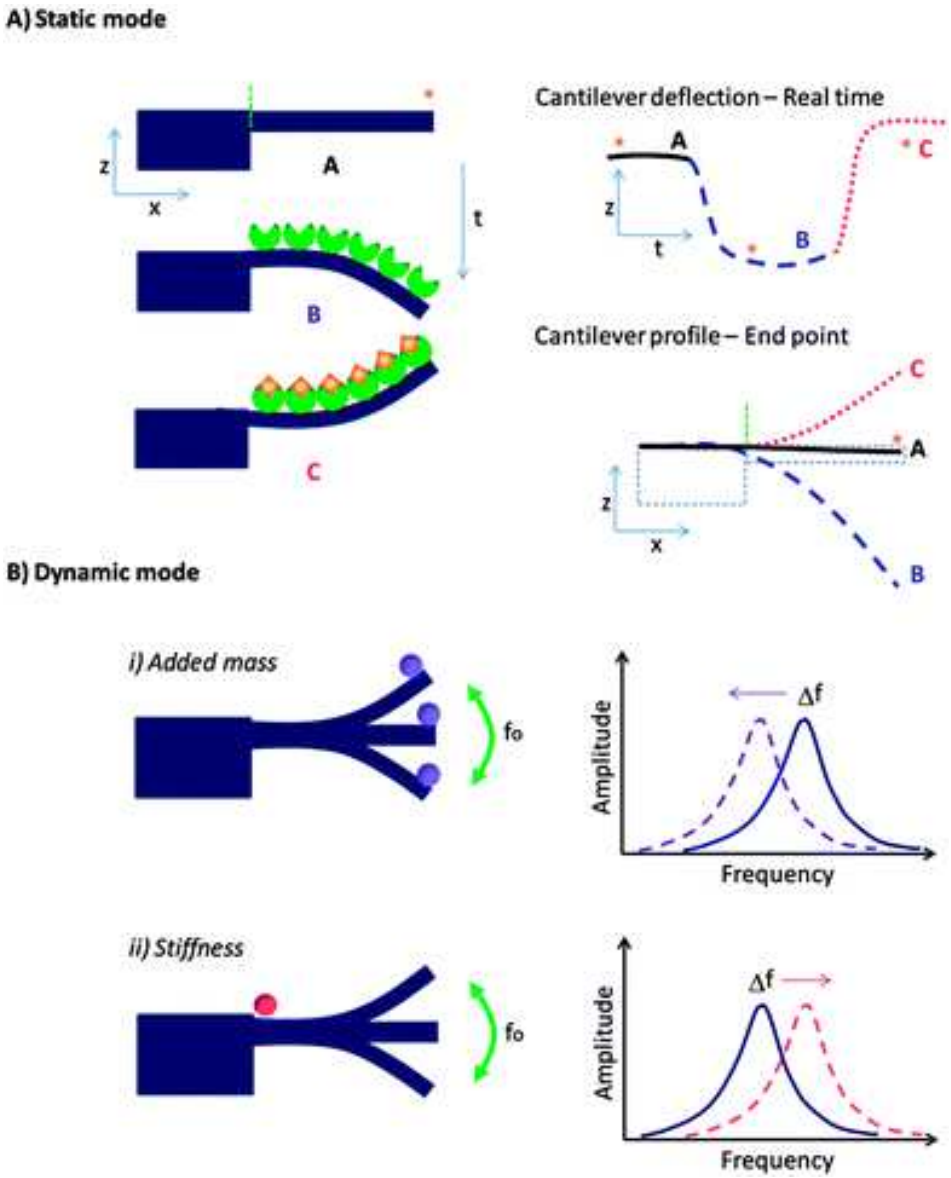

Mass sensing - an inverse problem

- This talk will focus on the detection of mass based on shift in frequency.
- Mass sensing is an inverse problem.
- The “answer” in general in non-unique. An added mass at a certain point on the sensor will produce an unique frequency shift. However, for a given frequency shift, there can be many possible combinations of mass values and locations.
- Therefore, predicting the frequency shift - the so called “forward problem” is not enough for sensor development.
- Advanced modelling and computation methods are available for the forward problem. However, they may not be always readily suitable for the inverse problem if the formulation is “complex” to start with.
- Often, a carefully formulated simplified computational approach could be more suitable for the inverse problem and consequently for reliable sensing.

The need for “instant” calculation

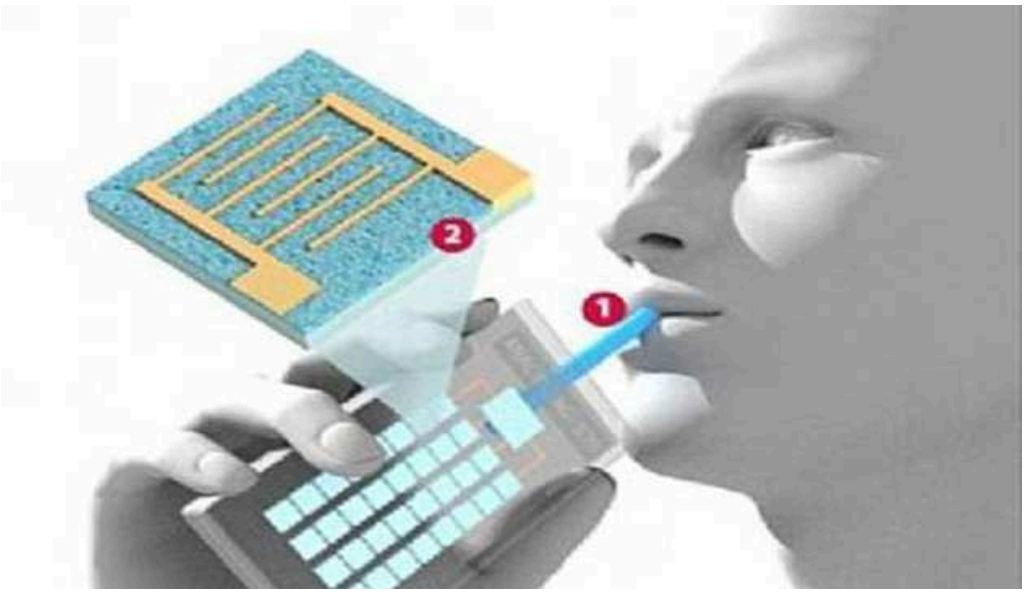

Sensing calculations must be performed very quickly - almost in real time with very little computational power (fast and cheap devices).

Single-walled carbon nanotube based sensors

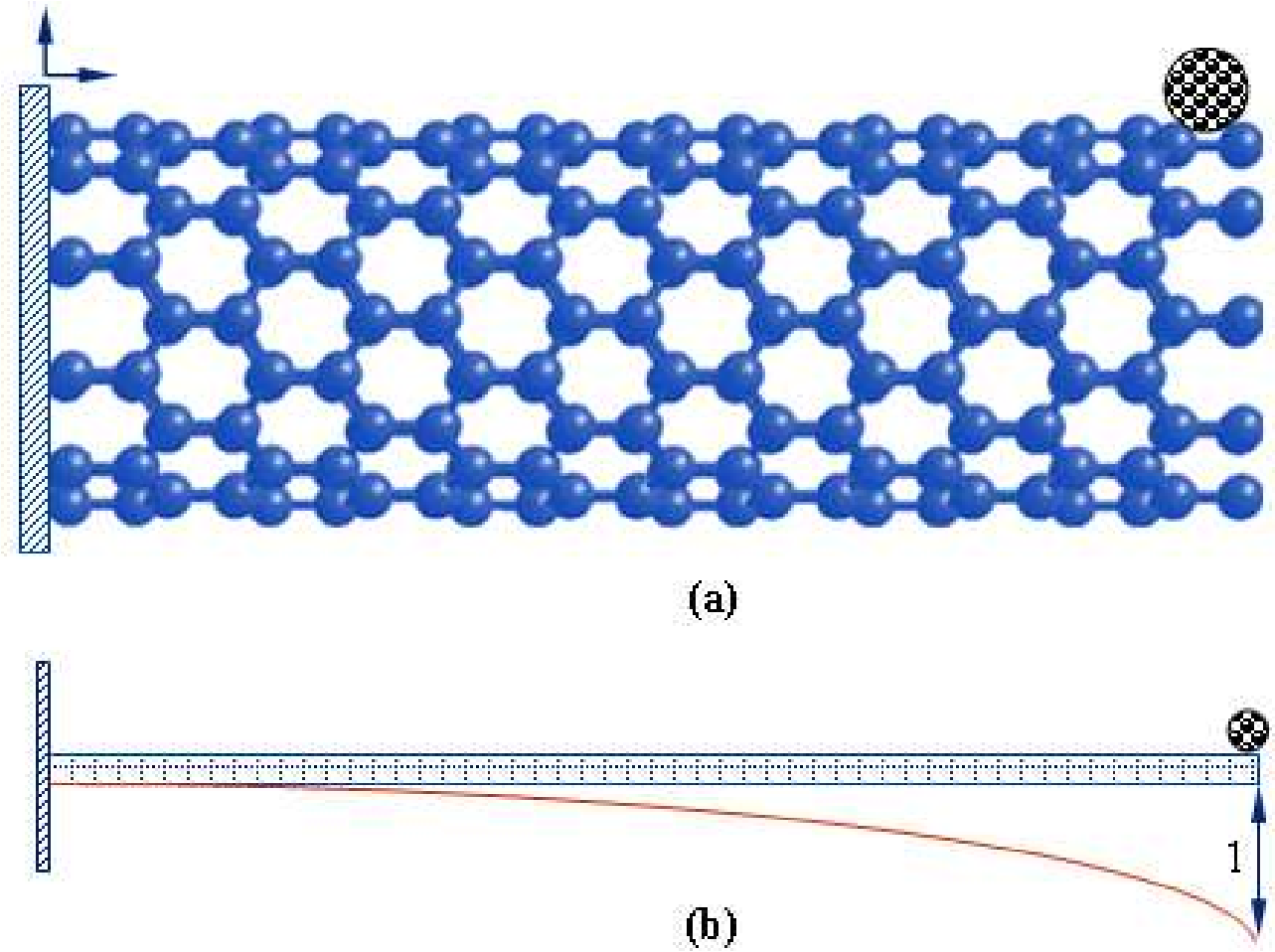

Cantilevered nanotube resonator with an attached mass at the tip of nanotube length: (a) Original configuration; (b) Mathematical idealization. Unit deflection under the mass is considered for the calculation of kinetic energy of the nanotube.

Single-walled carbon nanotube based sensors - bridged case

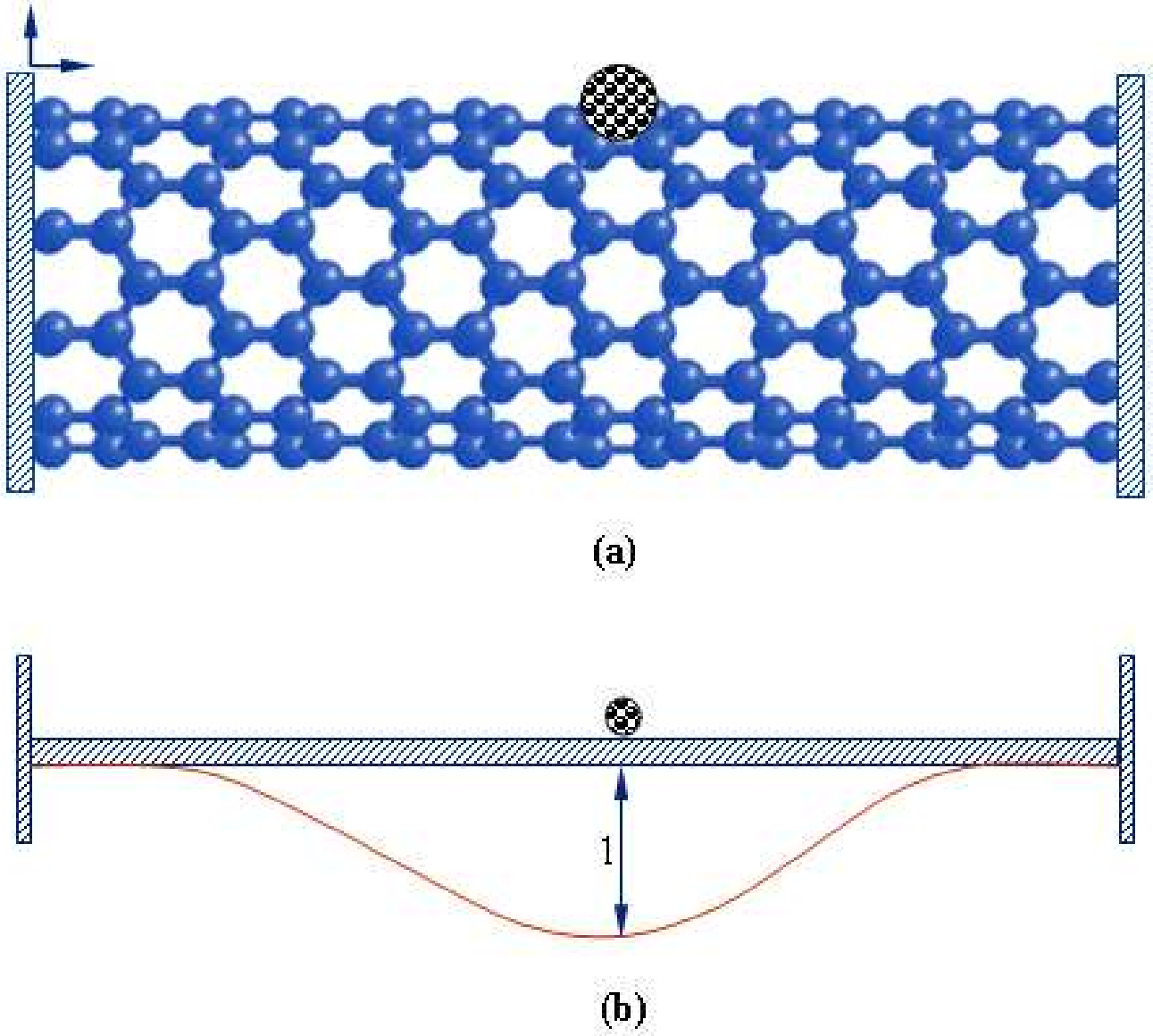

Bridged nanotube resonator with an attached mass at the center of nanotube

Resonant frequencies of SWCNT with attached mass

- In order to obtain simple analytical expressions of the mass of attached biochemical entities, we model a single walled CNT using a uniform beam based on classical Euler-Bernoulli beam theory:

$$EI\frac{\partial^4 y(x,t)}{\partial x^4} + \rho A\frac{\partial^2 y(x,t)}{\partial t^2} = 0 \tag{1}$$

where E the Youngs modulus, I the second moment of the cross-sectional area A, and ρ is the density of the material. Suppose the length of the SWCNT is L.

- Depending on the boundary condition of the SWCNT and the location of the attached mass, the resonant frequency of the combined system can be derived. We only consider the fundamental resonant frequency, which can be expresses as

$$f_n = \frac{1}{2\pi}\sqrt{\frac{k_{eq}}{m_{eq}}} \tag{2}$$

Here k_{eq} and m_{eq} are respectively equivalent stiffness and mass of SWCNT with attached mass in the first mode of vibration.

Cantilevered SWCNT with mass at the tip

- Suppose the value of the added mass is M. We give a virtual force at the location of the mass so that the deflection under the mass becomes unity. For this case $F_{eq} = 3EI/L^3$ so that

$$k_{eq} = \frac{3EI}{L^3} \tag{3}$$

- The deflection shape along the length of the SWCNT for this case can be obtained as

$$Y(x) = \frac{x^2\,(3\,L - x)}{2L^3} \tag{4}$$

- Assuming harmonic motion, i.e., $y(x,t) = Y(x)\exp(i\omega t)$, where ω is the frequency, the kinetic energy of the SWCNT can be obtained as

$$\begin{aligned} T &= \frac{\omega^2}{2}\int_0^L \rho A Y^2(x)dx + \frac{\omega^2}{2}MY^2(L) \\ &= \rho A\frac{\omega^2}{2}\int_0^L Y^2(x)dx + \frac{\omega^2}{2}M\,1^2 = \frac{\omega^2}{2}\left(\frac{33}{140}\rho AL + M\right) \end{aligned} \tag{5}$$

Cantilevered SWCNT with mass at the tip

- Therefore

$$m_{eq} = \frac{33}{140}\rho AL + M \tag{6}$$

- The resonant frequency can be obtained using equation (54) as

$$\begin{aligned} f_n &= \frac{1}{2\pi}\sqrt{\frac{k_{eq}}{m_{eq}}} = \frac{1}{2\pi}\sqrt{\frac{3EI/L^3}{\frac{33}{140}\rho AL + M}} \\ &= \frac{1}{2\pi}\sqrt{\frac{140}{11}}\sqrt{\frac{EI}{\rho AL^4}}\sqrt{\frac{1}{1+\frac{M}{\rho AL}\frac{140}{33}}} = \frac{1}{2\pi}\frac{\alpha^2\beta}{\sqrt{1+\Delta M}} \end{aligned} \tag{7}$$

where

$$\alpha^2 = \sqrt{\frac{140}{11}} \quad \text{or} \quad \alpha = 1.888 \tag{8}$$

$$\beta = \sqrt{\frac{EI}{\rho AL^4}} \tag{9}$$

$$\text{and} \quad \Delta M = \frac{M}{\rho AL}\mu, \quad \mu = \frac{140}{33} \tag{10}$$

Cantilevered SWCNT with mass at the tip

- Clearly the resonant frequency for a cantilevered SWCNT with no added tip mass is obtained by substituting $\Delta M = 0$ in equation (7) as

$$f_{0_n} = \frac{1}{2\pi}\alpha^2\beta \tag{11}$$

- Combining equations (7) and (11) one obtains the relationship between the resonant frequencies as

$$f_n = \frac{f_{0_n}}{\sqrt{1+\Delta M}} \tag{12}$$

General derivation of the sensor equations

- The frequency-shift can be expressed using equation (41) as

$$\Delta f = f_{0_n} - f_n = f_{0_n} - \frac{f_{0_n}}{\sqrt{1 + \Delta M}} \tag{13}$$

- From this we obtain

$$\frac{\Delta f}{f_{0_n}} = 1 - \frac{1}{\sqrt{1 + \Delta M}} \tag{14}$$

- Rearranging gives the expression

$$\Delta M = \frac{1}{\left(1 - \frac{\Delta f}{f_{0_n}}\right)^2} - 1 \tag{15}$$

- This equation completely relates the change is mass frequency-shift. Expanding equation (80) is Taylor series one obtains

$$\Delta M = \sum_j (j+1) \left(\frac{\Delta f}{f_{0_n}}\right)^j, \quad j = 1, 2, 3, \ldots \tag{16}$$

General derivation of the sensor equations

- Therefore, keeping upto first and third order terms one obtains the linear and cubic approximations as

$$\Delta M \approx 2\left(\frac{\Delta f}{f_{0_n}}\right) \tag{17}$$

$$\text{and} \quad \Delta M \approx 2\left(\frac{\Delta f}{f_{0_n}}\right) + 3\left(\frac{\Delta f}{f_{0_n}}\right)^2 + 4\left(\frac{\Delta f}{f_{0_n}}\right)^3 \tag{18}$$

- The actual value of the added mass can be obtained from (15) as

Mass detection from frequency shift

$$M = \frac{\rho A L}{\mu}\frac{\left(\alpha^2\beta\right)^2}{\left(\alpha^2\beta - 2\pi\Delta f\right)^2} - \frac{\rho A L}{\mu} \tag{19}$$

- Using the linear approximation, the value of the added mass can be obtained as

$$M = \frac{\rho A L}{\mu}\frac{2\pi\Delta f}{\alpha^2\beta} \tag{20}$$

Comparison of sensing results

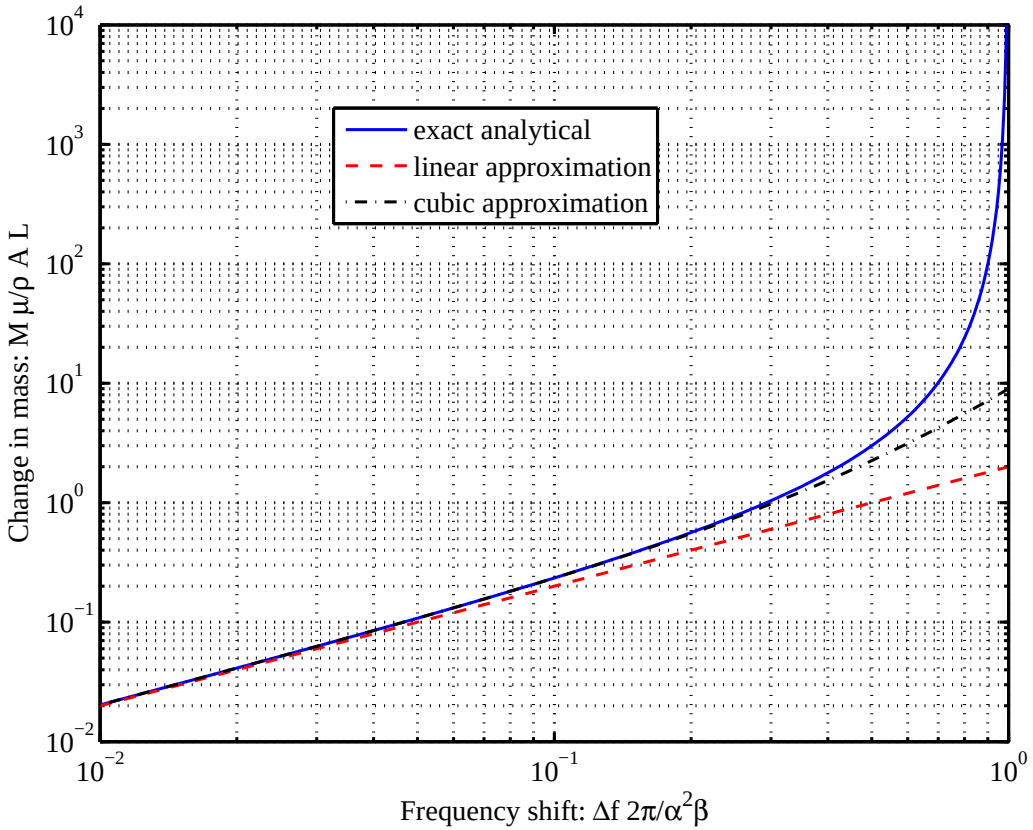

The general relationship between the normalized frequency-shift and normalized added mass of the bio-particles in a SWCNT with effective density ρ, cross-section area A and length L. Here $\beta = \sqrt{\frac{EI}{\rho AL^4}}\mathrm{s}^{-1}$, the nondimensional constant α depends on the boundary conditions and μ depends on the location of the mass. For a cantilevered SWCNT with a tip mass $\alpha^2 = \sqrt{140/11}$, $\mu = 140/33$ and for a bridged SWCNT with a mass at the midpoint $\alpha^2 = \sqrt{6720/13}$, $\mu = 35/13$.

Validation of sensor equations - FE model

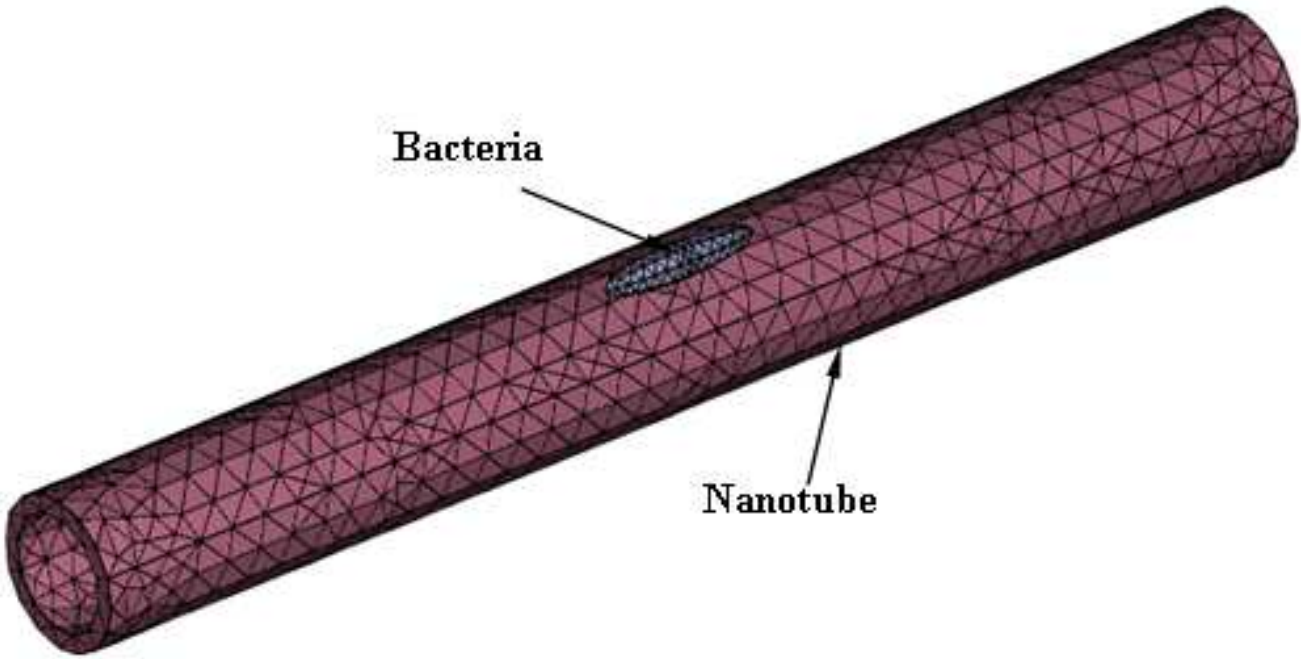

The theory of linear elasticity is used for both the CNT and the bacteria. FE model: number of degrees of freedom $= 55401$, number of mesh point $= 2810$, number of elements (tetrahedral element) $= 10974$, number of boundary elements (triangular element) $= 3748$, number of vertex elements $= 22$, number of edge elements $= 432$, minimum element quality $= 0.2382$ and element volume ratio $= 0.0021$. Length of the nanotube is 8 nm and length of bacteria is varied between 0.5 to 3.5 nm.

Validation of sensor equations - model data

Table: Geometrical and material properties for the single-walled carbon nanotube and the bacterial mass.

SWCNT	Bacteria (E Coli)
$L = 8$ nm	$E = 25.0MPa$
$E = 1.0TPa$	$\rho = 1.16g/cc$
$\rho = 2.24g/cc$	–
$D = 1.1nm$	–
$\nu = 0.30nm$	–

Validation of sensor equations - frequency values

Table: Comparison of frequencies (100 GHz) obtained from finite element simulation with MD simulation for the bridged configuration. For the 8.0 nm SWCNT used in this study, the maximum error is less than about 4%.

D(nm)	L(nm)		f_1	f_2	f_3	f_4	f_5
		MD	10.315	10.315	10.478	10.478	15.796
	4.1	*FE*	10.769	10.769	16.859	22.224	22.224
		%error	-4.40	-4.40	-60.90	-112.10	-40.69
		MD	6.616	6.616	9.143	9.143	11.763
1.1	5.6	*FE*	6.883	6.884	12.237	14.922	14.924
		%error	-4.04	-4.05	-33.84	-63.21	-26.87
		MD	3.800	3.8	8.679	8.679	8.801
	8.0	*FE*	3.900	3.9	8.659	9.034	9.034
		%error	-2.63	-2.63	-0.23	-4.09	-2.65

Validation of sensor equations - Cantilever nanotube

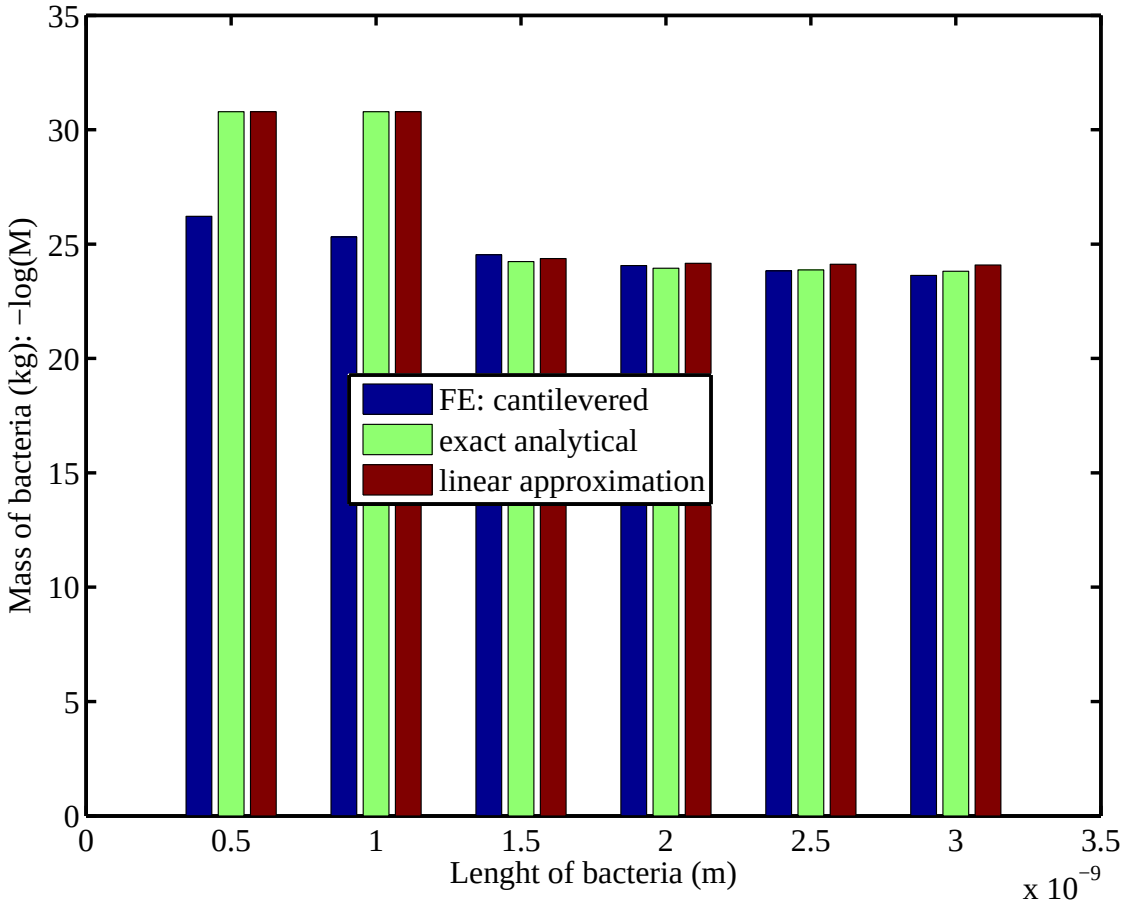

The variation of identified mass with bacterial length using the finite element simulation, exact analytical formula and the linear approximation for the cantilevered nanotube. Proposed analytical expressions are in good agreement with the detailed finite element results for longer bacterial length.

Validation of sensor equations - Bridged nanotube

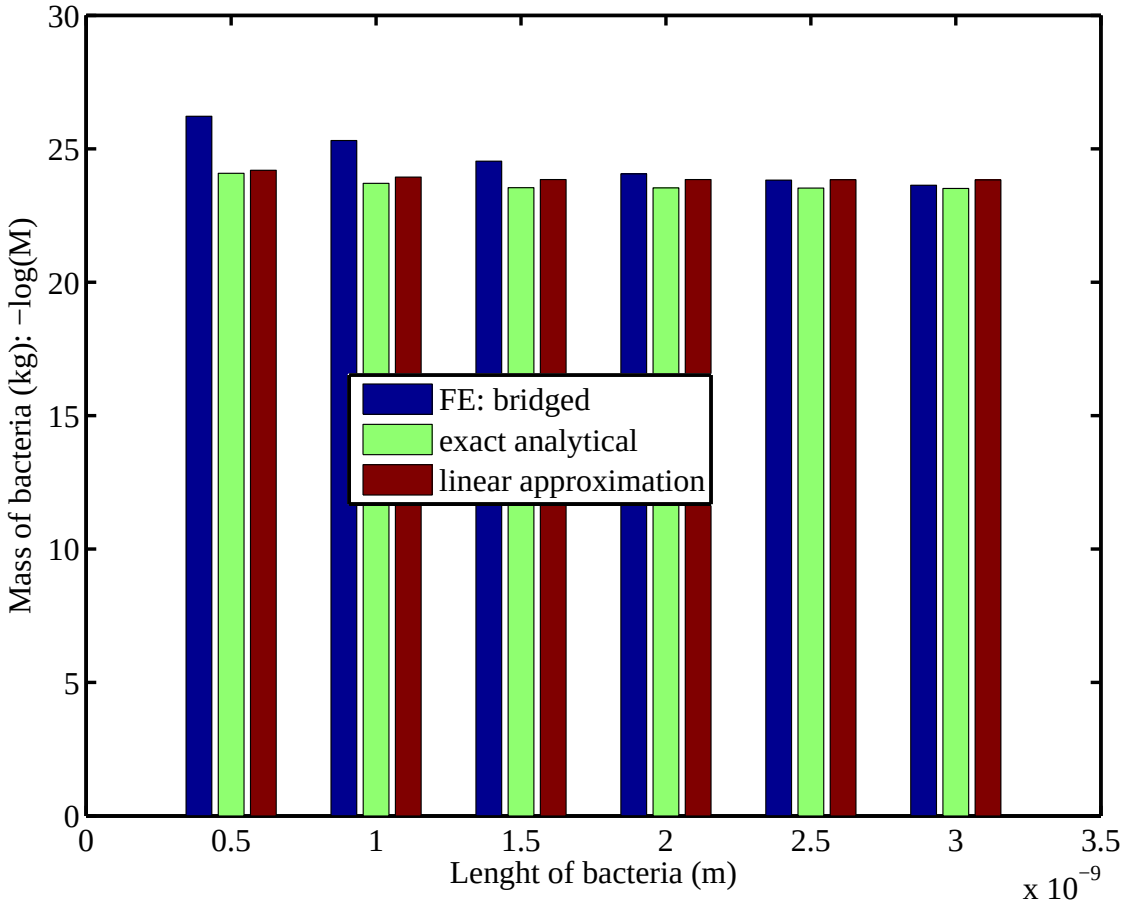

The variation of identified mass with bacterial length using the finite element simulation, exact analytical formula and the linear approximation for the bridged nanotube. Proposed analytical expressions are in good agreement with the detailed finite element results for longer bacterial length.

Validation of sensor equations

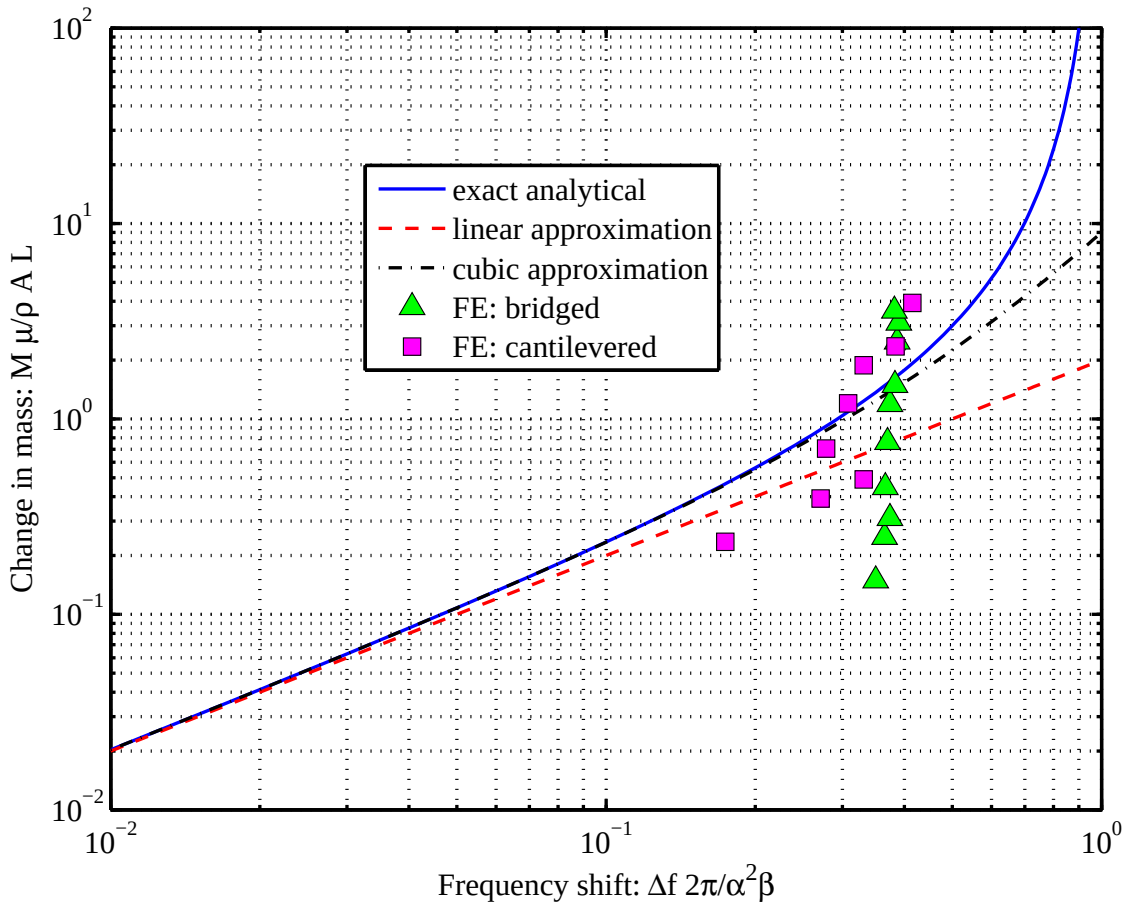

The general relationship between the normalized frequency-shift and normalized added mass of the bio-particles in a SWCNT with effective density ρ, cross-section area A and length L. Relationship between the frequency-shift and added mass of bio-particles obtained from finite element simulation are also presented here to visualize the effectiveness of analytical formulas.

Dynamic theory of CNT

- For the cantilevered CNT, the resonance frequencies can be obtained from

$$f_j = \frac{\lambda_j^2}{2\pi}\sqrt{\frac{EI}{\rho A L^4}} \tag{21}$$

where λ_j can be obtained by solving the following transcendental equation

$$\cos\lambda\cosh\lambda + 1 = 0 \tag{22}$$

- The vibration mode shape can be expressed as

$$Y_j(\xi) = \left(\cosh\lambda_j\xi - \cos\lambda_j\xi\right) - \left(\frac{\sinh\lambda_j - \sin\lambda_j}{\cosh\lambda_j + \cos\lambda_j}\right)\left(\sinh\lambda_j\xi - \sin\lambda_j\xi\right) \tag{23}$$

where

$$\xi = \frac{x}{L} \tag{24}$$

is the normalized coordinate along the length of the CNT. For sensing applications we are interested in the first mode of vibration for which $\lambda_1 = 1.8751$.

Cantilevered nanotube resonator with attached masses (DeOxy Thymidine)

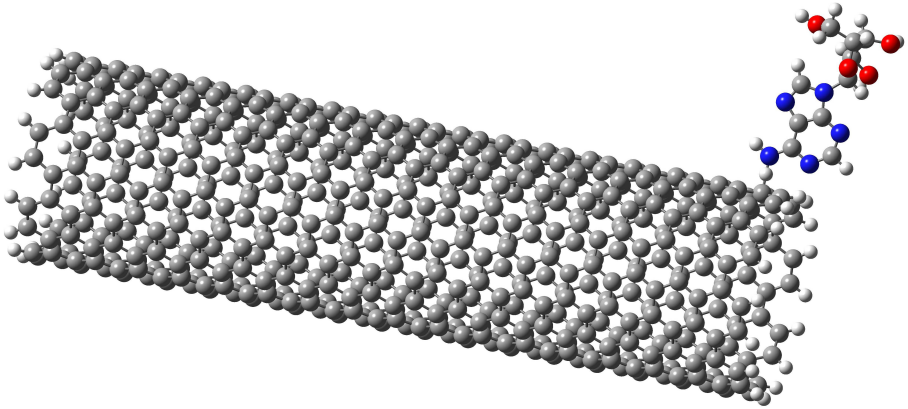

(a) DeOxy Thymidine at the edge of a SWCNT

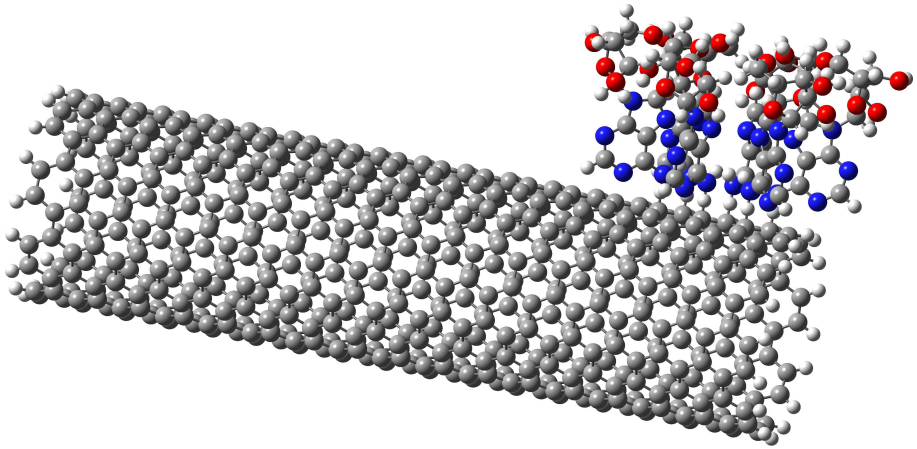

(b) DeOxy Thymidine distributed over the length of a SWCNT

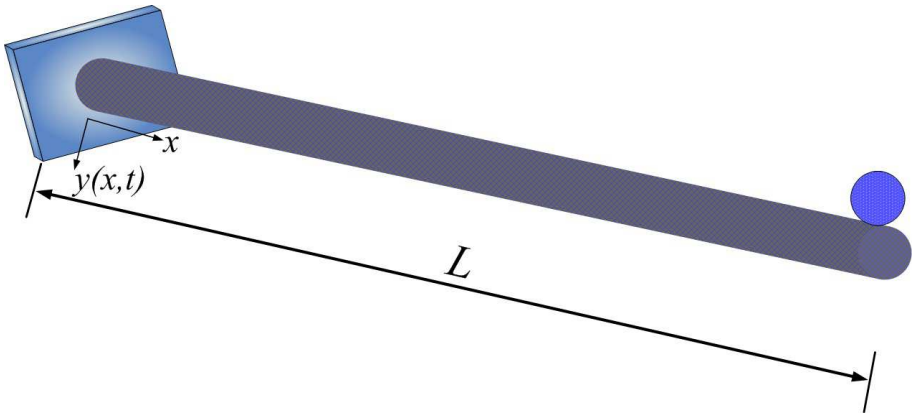

(c) Mathematical idealization of (a): point mass at the tip

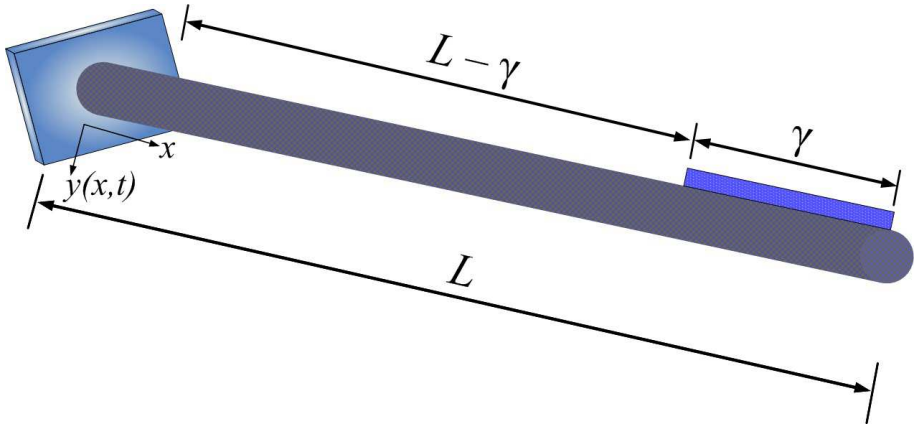

(d) Mathematical idealization of (b): distributed mass along the length

Exact dynamic solution

- Suppose there is an attached nano/bio object of mass M at the end of the cantilevered resonator in 1(a). The boundary conditions with an additional mass of M at $x = L$ can be expressed as

$$y(0,t) = 0, \quad y'(0,t) = 0, \quad y''(L,t) = 0,$$
$$\text{and} \quad EIy'''(L,t) - M\ddot{y}(L,t) = 0 \tag{25}$$

- Here $(\bullet)'$ denotes derivative with respective to x and $(\dot{\bullet})$ denotes derivative with respective to t. Assuming harmonic solution $y(x,t) = Y(x)e^{i\omega t}$ and using the boundary conditions, it can be shown that the resonance frequencies are still obtained from Eq. (21) but λ_j should be obtained by solving

$$(\cos\lambda \sinh\lambda - \sin\lambda \cosh\lambda)\,\Delta M\,\lambda + (\cos\lambda \cosh\lambda + 1) = 0 \tag{26}$$

Here

$$\Delta M = \frac{M}{\rho AL} \tag{27}$$

is the ratio of the added mass and the mass of the CNT. If the added mass is zero, then one can see that Eq. (27) reduces to Eq. (22).

Calibration Constants - energy approach

- These equations are obtained by considering the differential equation and the boundary conditions in an exact manner.
- They are complex enough so that a simple relationship between the change in the mass and the shift in frequency is not available.
- Moreover, these equations are valid for point mass only. Many biological objects are relatively large in dimension and therefore the assumption that the mass is concentrated at one point may not be valid.
- In the fundamental mode of vibration, the natural frequency of a SWCNT oscillator can be expressed as

$$f_n = \frac{1}{2\pi}\sqrt{\frac{k_{eq}}{m_{eq}}} \tag{28}$$

  Here k_{eq} and m_{eq} are respectively equivalent stiffness and mass of SWCNT in the first mode of vibration.
- The equivalent mass m_{eq} changes depending on whether a nano-object is attached to the CNT. This in turn changes the natural frequency.

Calibration Constants - energy approach

- Suppose Y_j is the assumed displacement function for the first mode of vibration.
- Suppose the added mass occupies a length γL and its mass per unit length is m. Therefore, $M = m \times \gamma L$. From the kinetic energy of the SWCNT with the added mass and assuming harmonic motion, the overall equivalent mass m_{eq} can be expressed as

$$m_{eq} = \rho AL \underbrace{\int_0^1 Y_j^2(\xi)\mathrm{d}\xi}_{I_1} + M \underbrace{\int_\Gamma Y_j^2(\xi)\mathrm{d}\xi}_{I_2} \tag{29}$$

where Γ is the domain of the additional mass. From the potential energy, the equivalent stiffness k_{eq} can be obtained as

$$k_{eq} = \frac{EI}{L^3} \underbrace{\int_0^1 Y_j''^2(\xi)\mathrm{d}\xi}_{I_3} \tag{30}$$

Calibration Constants - energy approach

- From these expressions we have

$$\frac{k_{eq}}{m_{eq}} = \frac{EI/L^3\, I_3}{\rho A L I_1 + M I_2} = \left(\frac{EI}{\rho A L^4}\right) \frac{I_3}{I_1 + I_2 \Delta M} \tag{31}$$

where the mass ratio ΔM is defined in Eq. (27). Using the expression of the natural frequency we have

$$f_n = \frac{1}{2\pi}\sqrt{\frac{k_{eq}}{m_{eq}}} = \frac{\beta}{2\pi}\frac{c_k}{\sqrt{1 + c_m \Delta M}} \tag{32}$$

where $\beta = \sqrt{\frac{EI}{\rho A L^4}}$

- The stiffness and mass calibration constants are

$$c_k = \sqrt{\frac{I_3}{I_1}} \quad \text{and} \quad c_m = \frac{I_2}{I_1} \tag{33}$$

- Equation (32), together with the calibration constants gives an explicit relationship between the change in the mass and frequency.

Calibration Constants - point mass

- We fist consider the cantilevered CNT with an added point mass. For the cantilevered CNT, we use the mode shape in (23) as the assumed deflection shape Y_j. The value of λ_j appearing in this equation is 1.8751. Using these the integral I_1 can be obtained as

$$I_1 = \int_0^1 Y_j^2(\xi)\mathrm{d}\xi = 1.0 \tag{34}$$

- For the point mass at the end of the cantilevered SWNT we have

$$m(\xi) = M\delta(\xi - 1) \tag{35}$$

- Using these, the integral I_2 can be obtained as

$$I_2 = \int_0^1 \delta(\xi - 1)\, Y_j^2(\xi)\mathrm{d}\xi = Y_j^2(1) = 4.0 \tag{36}$$

- Differentiating $Y_j(\xi)$ in Eq. (23) with respect to ξ twice, we obtain

$$I_3 = \int_0^1 Y_j^{''2}(\xi)\mathrm{d}\xi = 12.3624 \tag{37}$$

Calibration Constants - distributed mass

- Using these integrals, the stiffness and mass calibration factors can be obtained as

$$c_k = \sqrt{\frac{I_3}{I_1}} = 3.5160 \quad \text{and} \quad c_m = \frac{I_2}{I_1} = 4.0 \tag{38}$$

- Now we consider the case when the mass is distributed over a length γL from the edge of the cantilevered CNT. Since the total mass is M, the mass per unit length is $M/\gamma L$. Noting that the added mass is between $(1-\gamma)L$ to L, the integral I_2 can be expressed as

$$I_2 = \frac{1}{\gamma}\int_{\xi=1-\gamma}^{1} Y_j^2(\xi)\mathrm{d}\xi; \quad 0 \leq \gamma \leq 1 \tag{39}$$

This integral can be calculated for different values of γ.

Calibration Constants - non-dimensional values

Table: The stiffness (c_k) and mass (c_m) calibration constants for CNT based bio-nano sensor. The value of γ indicates the length of the mass as a fraction of the length of the CNT.

Mass size	Cantilevered CNT		Bridged CNT	
	c_k	c_m	c_k	c_m
Point mass ($\gamma \to 0$)	3.5160152	4.0	22.373285	2.522208547
$\gamma = 0.1$		3.474732666		2.486573805
$\gamma = 0.2$		3.000820053		2.383894805
$\gamma = 0.3$		2.579653837		2.226110255
$\gamma = 0.4$		2.212267400		2.030797235
$\gamma = 0.5$		1.898480438		1.818142650
$\gamma = 0.6$		1.636330135		1.607531183
$\gamma = 0.7$		1.421839146		1.414412512
$\gamma = 0.8$		1.249156270		1.248100151

Sensor equation based on calibration constants

- The resonant frequency of a SWCNT with no added mass is obtained by substituting $\Delta M = 0$ in Eq. (32) as

$$f_{0_n} = \frac{1}{2\pi} c_k \beta \tag{40}$$

- Combining equations (32) and (40) one obtains the relationship between the resonant frequencies as

$$f_n = \frac{f_{0_n}}{\sqrt{1 + c_m \Delta M}} \tag{41}$$

- The frequency-shift can be expressed using Eq. (41) as

$$\Delta f = f_{0_n} - f_n = f_{0_n} - \frac{f_{0_n}}{\sqrt{1 + c_m \Delta M}} \tag{42}$$

- From this we obtain

$$\frac{\Delta f}{f_{0_n}} = 1 - \frac{1}{\sqrt{1 + c_m \Delta M}} \tag{43}$$

Sensor equation based on calibration constants

- Rearranging gives the expression

Relative mass detection

$$\Delta M = \frac{1}{c_m \left(1 - \frac{\Delta f}{f_{0_n}}\right)^2} - \frac{1}{c_m} \tag{44}$$

- This equation completely relates the change in mass with the frequency-shift using the mass calibration constant. The actual value of the added mass can be obtained from (44) as

Absolute mass detection

$$M = \frac{\rho A L}{c_m} \frac{\left(c_k^2 \beta^2\right)}{\left(c_k \beta - 2\pi \Delta f\right)^2} - \frac{\rho A L}{c_m} \tag{45}$$

This is the general equation which completely relates the added mass and the frequency shift using the calibration constants.

Validation based on molecular mechanics simulation

- In the calculation, GAUSSIAN 09 computer software and the universal force field (UFF) developed by Rappe et al. are employed.
- The universal force field is a harmonic force field, in which the general expression of total energy is a sum of energies due to valence or bonded interactions and non-bonded interactions

$$E = \sum E_R + \sum E_\theta + \sum E_\phi + \sum E_\omega + \sum E_{VDW} + \sum E_{el} \qquad (46)$$

  The valence interactions consist of bond stretching (E_R) and angular distortions.
- The angular distortions are bond angle bending (E_θ), dihedral angle torsion (E_ϕ) and inversion terms (E_ω). The non-bonded interactions consist of van der Waals (E_{VDW}) and electrostatic (E_{el}) terms.
- We used UFF model, wherein the force field parameters are estimated using general rules based only on the element, its hybridization and its connectivity.

Comparison with MD simulations

Table: Natural frequencies of a (5,5) carbon nanotube in THz - Cantilever boundary condition. First four natural frequencies obtained from the present approach is compared with the MD simulation [Duan et al, 2007 - J. App. Phy] for different values of the aspect ratio.

Aspect Ratio	Present analysis				MD simulation			
	1st	2nd	3rd	4th	1st	2nd	3rd	4th
5.26	0.220	1.113	2.546	4.075	0.212	1.043	2.340	3.682
5.62	0.195	1.005	2.325	3.759	0.188	0.943	2.141	3.406
5.99	0.174	0.912	2.132	3.478	0.167	0.857	1.967	3.158
6.35	0.156	0.830	1.961	3.226	0.150	0.782	1.813	2.936
6.71	0.141	0.759	1.810	3.000	0.136	0.716	1.676	2.736
7.07	0.128	0.696	1.675	2.797	0.123	0.657	1.553	2.555
7.44	0.116	0.641	1.554	2.614	0.112	0.605	1.443	2.392
7.80	0.106	0.592	1.446	2.447	0.102	0.559	1.344	2.243
8.16	0.098	0.548	1.348	2.296	0.094	0.518	1.255	2.108
8.52	0.089	0.492	1.231	2.102	0.086	0.481	1.174	1.984

Zigzag (5,0) SWCNT of length 8.52 nm with added DeOxy Thymidine (a nucleotide that is found in DNA)

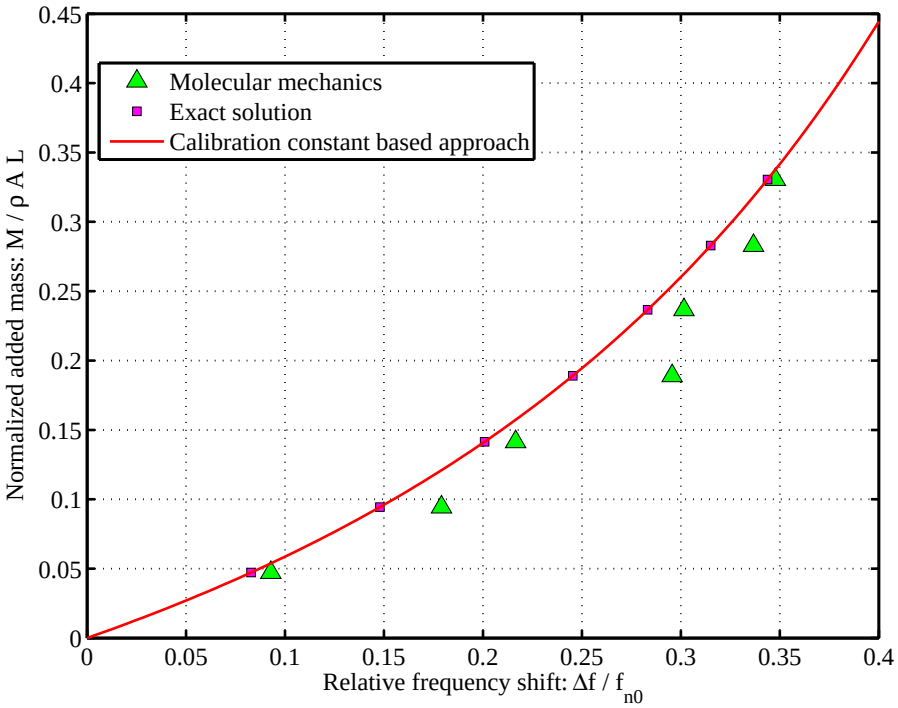

(a) Point mass on a cantilevered CNT.

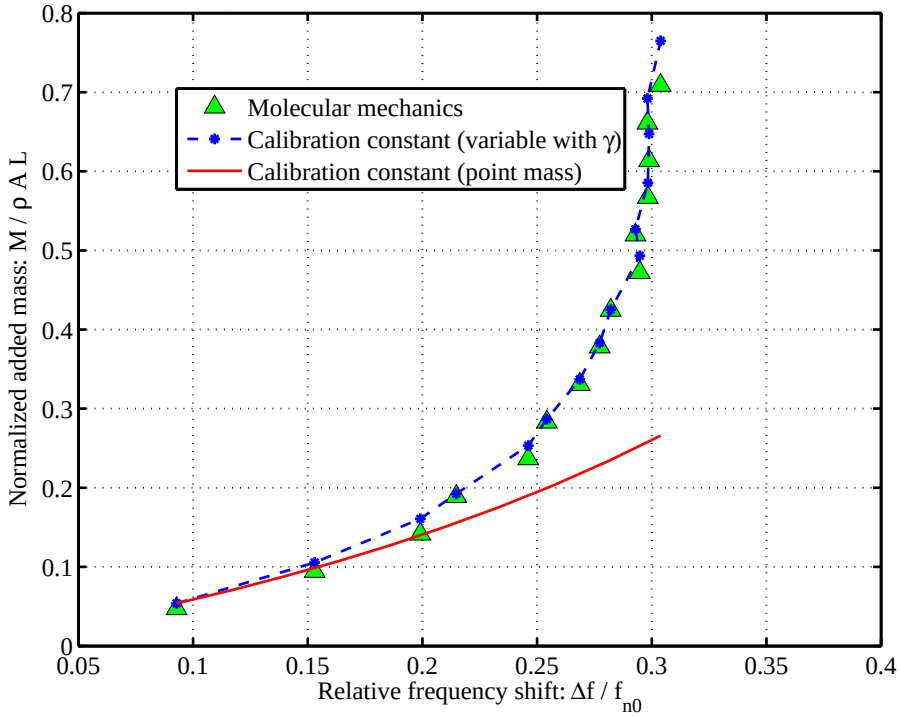

(b) Distributed mass on a cantilevered CNT. The length of the mass varies between $0.05L$ to $0.72L$ from the edge of the CNT.

Figure: Identified attached masses from the frequency-shift of a cantilevered CNT. The proposed calibration constant based approach is validated using data from the molecular mechanics simulations. The importance of using the calibration constant varying with the length of the mass can be seen in (b). The point mass assumption often used in cantilevered sensors, can result in significant error when the mass is distributed in nature.

Error in mass detection

Point mass	
Relative frequency shift	% error
0.0929	13.9879
0.1790	28.1027
0.2165	11.1765
0.2956	34.2823
0.3016	10.9296
0.3367	12.4422
0.3477	2.1427

Distributed mass		
Relative frequency shift	Normalized length	% error
0.0929	0	13.9879
0.1530	0.0500	11.8626
0.1991	0.1000	13.7038
0.2148	0.1500	1.7865
0.2462	0.2000	7.0172
0.2542	0.2500	1.3278
0.2687	0.3000	1.9943
0.2773	0.3500	1.2631
0.2821	0.4000	0.1653
0.2948	0.4500	4.5150
0.2929	0.5000	1.3776
0.2983	0.5500	3.2275
0.2989	0.6167	5.5240
0.2981	0.6667	4.6735
0.3039	0.7167	7.9455

Bridged nanotube resonator with attached masses (DeOxy Thymidine)

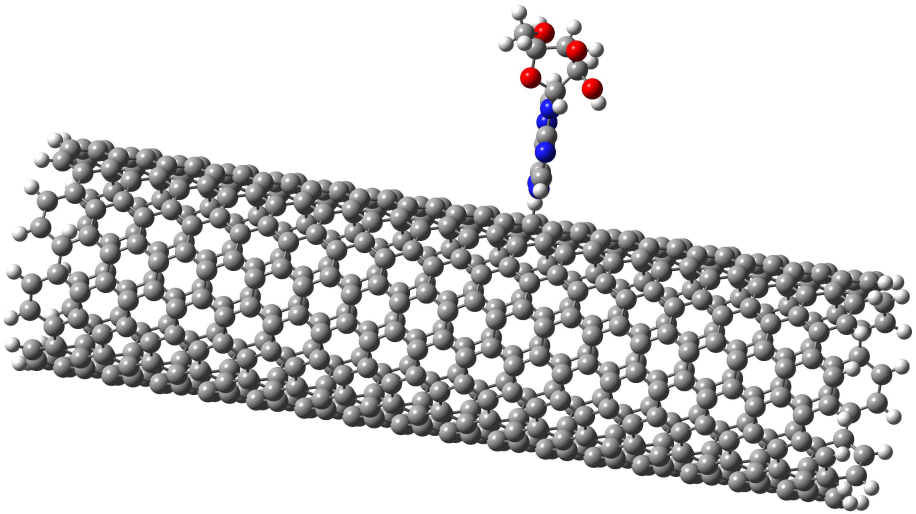

(a) DeOxy Thymidine at the centre of a SWCNT

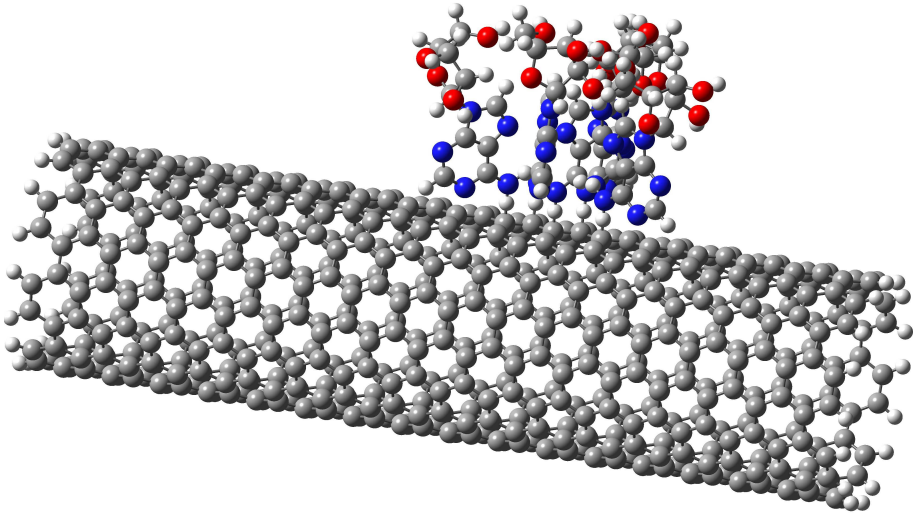

(b) DeOxy Thymidine distributed about the centre of a SWCN

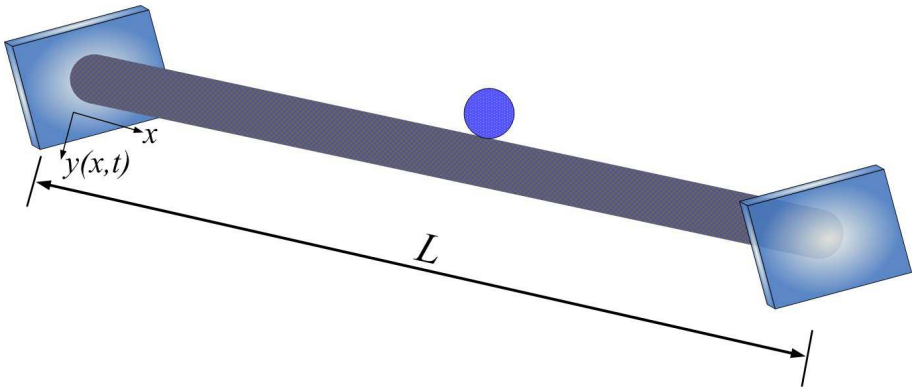

(c) Mathematical idealization of (a): point mass at the centre

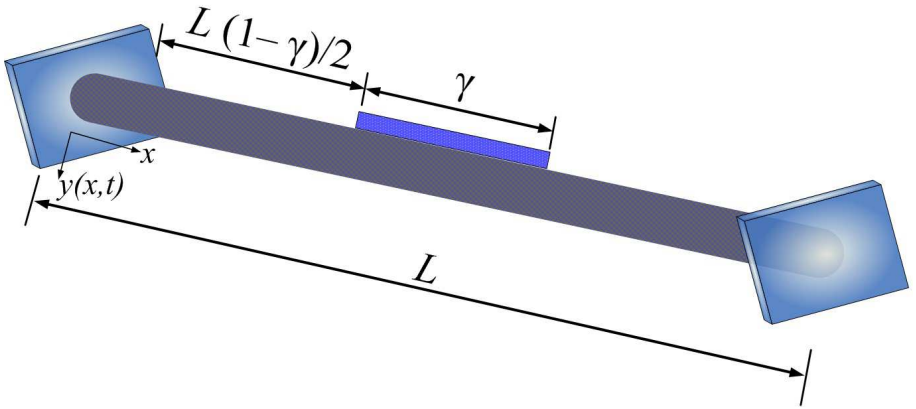

(d) Mathematical idealization of (b): distributed mass about the centre

Zigzag (5,0) SWCNT of length 8.52 nm with added DeOxy Thymidine (a nucleotide that is found in DNA)

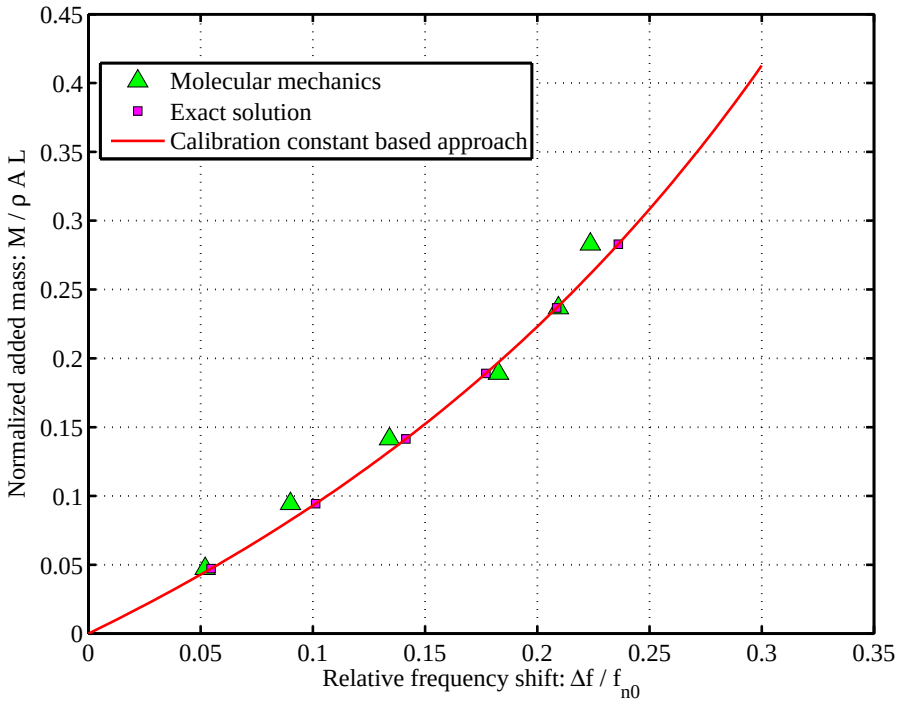

(a) Point mass on a bridged CNT.

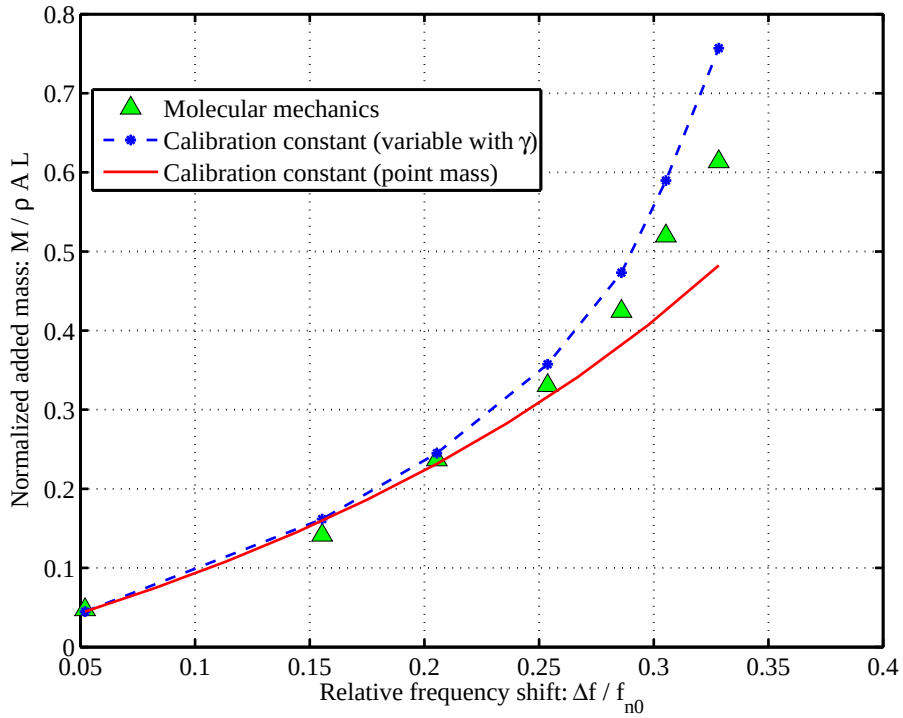

(b) Distributed mass on a bridged CNT. The length of the mass varies between $0.1L$ to $0.6L$ about the centre of the CNT.

Figure: Identified attached masses from the frequency-shift of a bridged CNT. The proposed calibration constant based approach is validated using data from the molecular mechanics simulations. Again, the importance of using the calibration constant varying with the length of the mass can be seen in (b). However, the difference between the point mass and distributed mass assumption is not as significant as the cantilevered case.

Error in mass detection

Point mass		Distributed mass		
Relative frequency shift $(\Delta f / f_{0_n})$	% error	Relative frequency shift $(\Delta f / f_{0_n})$	Normalized length (γ)	% error
0.0521	5.1632	0.0521	0	5.1636
0.0901	12.7402	0.1555	0.1000	14.2792
0.1342	6.4153	0.2055	0.2000	3.5290
0.1827	4.2630	0.2538	0.3000	8.1455
0.2094	0.5273	0.2859	0.4000	11.5109
0.2237	7.6267	0.3053	0.5000	13.4830
		0.3284	0.6000	23.3768

Simulation methods

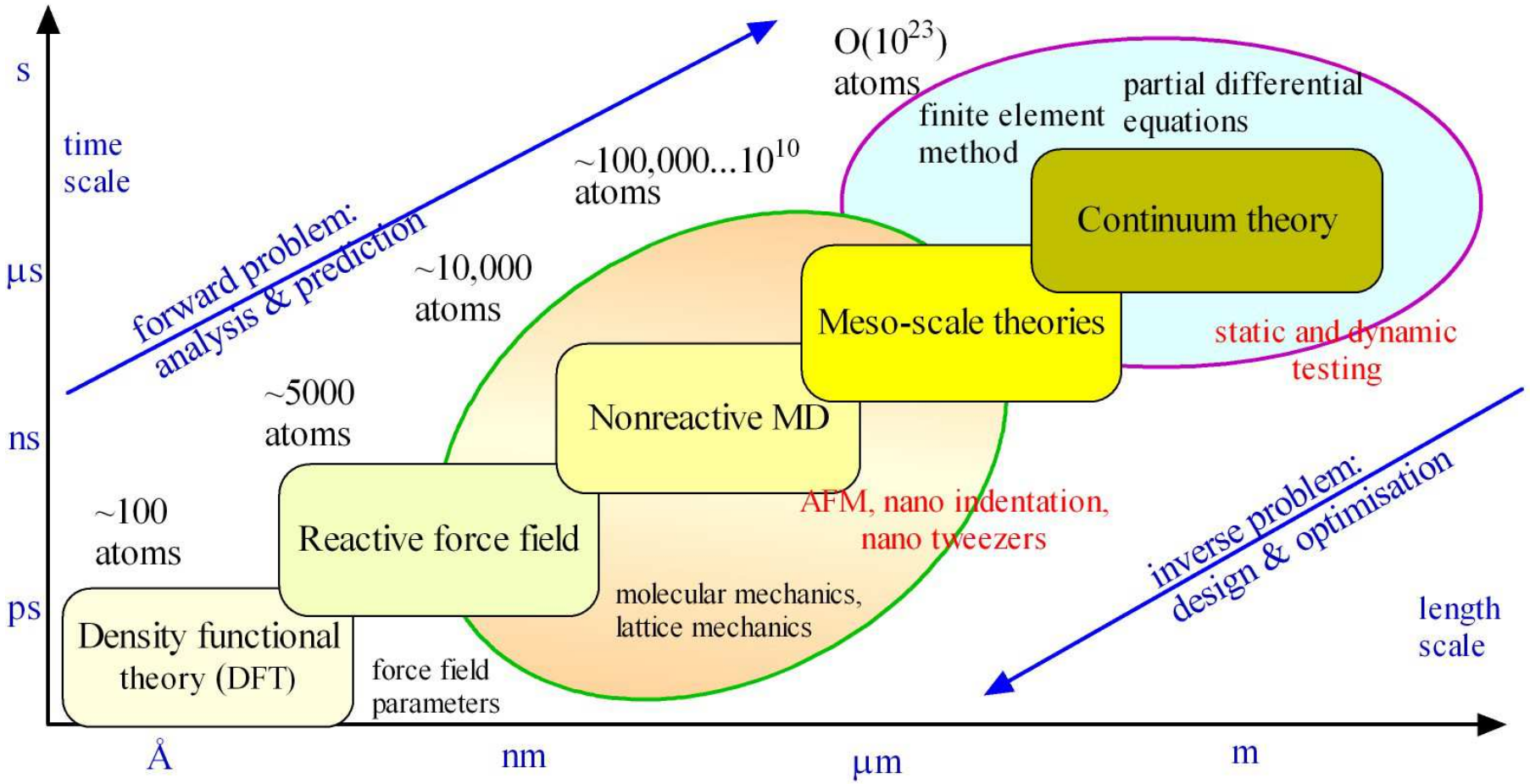

Continuum mechanics at the nanoscale

- Experiments at the nanoscale are generally difficult at this point of time.
- On the other hand, atomistic computation methods such as molecular dynamic (MD) simulations are computationally prohibitive for nanostructures with large numbers of atoms.
- Continuum mechanics can be an important tool for modelling, understanding and predicting physical behaviour of nanostructures.
- Although continuum models based on classical elasticity are able to predict the general behaviour of nanostructures, they often lack the accountability of effects arising from the small-scale.
- To address this, size-dependent continuum based methods are gaining in popularity in the modelling of small sized structures as they offer much faster solutions than molecular dynamic simulations for various nano engineering problems.
- Currently research efforts are undergoing to bring in the size-effects within the formulation by modifying the traditional classical mechanics.

Nonlocal continuum mechanics

- One popularly used size-dependant theory is the nonlocal elasticity theory pioneered by Eringen [1983], and has been applied to nanotechnology.
- Nonlocal continuum mechanics is being increasingly used for efficient analysis of nanostructures viz. nanorods, nanobeams, nanoplates, nanorings, carbon nanotubes, graphenes, nanoswitches and microtubules. Nonlocal elasticity accounts for the small-scale effects at the atomistic level.
- In the nonlocal elasticity theory, according to Eringen [1983], the small-scale effects are captured by assuming that the stress at a point as a function of the strains at all points in the domain.
- Nonlocal theory considerslong-range inter-atomic interactions and yields results dependent on the size of a body.
- Some of the drawbacks of the classical continuum theory could be efficiently avoided and size-dependent phenomena can be explained by the nonlocal elasticity theory.

Nonlocal continuum mechanics

- The basic equations for a nonlocal isotropic linear homogenous elastic body can be expresses as

$$\begin{aligned} \sigma_{ij,j} &= 0, \\ \sigma_{ij}(\mathbf{x}) &= \int_V \phi(|\mathbf{x}-\mathbf{x}'|,\alpha)\mathbf{t}_{ij}d\mathbf{V}(\mathbf{x}'), \quad \forall x \in \mathbf{V} \\ \mathbf{t}_{ij} &= H_{ijkl}\epsilon_{kl}, \\ \epsilon_{ij} &= 1/2(u_{i,j}+u_{j,i} \end{aligned} \tag{47}$$

- The terms σ_{ij}, t_{ij}, ϵ_{kl} and H_{ijkl} are the nonlocal stress, classical stress, classical strain and fourth-order elasticity tensors respectively. The volume integral is over the region **V** occupied by the body. Equation (47) couples the stress due to nonlocal elasticity and the stress due to classical elasticity.
- The kernel function $\phi(|\mathbf{x}-\mathbf{x}'|,\alpha)$ is the nonlocal modulus. The nonlocal modulus acts as an attenuation function incorporating into constitutive equations the nonlocal effects at the reference point **x** produced by local strain at the source $\mathbf{x}'$.

Nonlocal continuum mechanics

- The term $|\mathbf{x} - \mathbf{x}'|$ represents the distance in the Euclidean form and α is a material constant that depends on the internal (e.g. lattice parameter, granular size, distance between the C-C bonds) and external characteristics lengths (e.g. crack length, wave length).
- Material constant α is defined as $\alpha = (e_0 a)/l$. Here e_0 is a constant for calibrating the model with experimental results and other validated models. The parameter e_0 is estimated such that the relations of the nonlocal elasticity model could provide satisfactory approximation to the atomic dispersion curves of the plane waves with those obtained from the atomistic lattice dynamics.
- The terms a and l are the internal (e.g. lattice parameter, granular size, distance between C-C bonds) and external characteristics lengths (e.g. crack length, wave length) of the nanostructure. Equation (47) effectively shows that in nonlocal theory, the stress at a point is a function of the strains at all points in the domain. The classical elasticity can be viewed as a special cade when the kernel function becomes a Dirac delta function.

Nonlocal continuum mechanics

- The direct use of equation (47) in boundary value problems results in integro-partial differential equations and they are generally difficult to solve analytically.
- For this reason, a differential form of nonlocal elasticity equation is often beneficial. According to Eringen this can be achieved for a special case of the kernel function given by

$$\phi(|x - x'|, \alpha) = (2\pi\ell^2\alpha^2)K_0(\sqrt{x \bullet x}/\ell\alpha) \tag{48}$$

- Here K_0 is the modified Bessel function. The equation of motion in terms of nonlocal elasticity can be expressed as

$$\sigma_{ij,j} + f_i = \rho\ddot{u}_i \tag{49}$$

where f_i, ρ and u_i are the components of the body forces, mass density, and the displacement vector, respectively.

Nonlocal continuum mechanics

- The terms i, j takes up the symbols x, y, and z. The operator $(\ddot{\bullet})$ denotes double derivative with respect to time. Assuming the kernel function ϕ as the Green's function, Eringen proposed a differential form of the nonlocal constitutive relation as

$$\sigma_{ij,j} + \mathcal{L}(f_i - \rho \ddot{u}_i) = 0 \tag{50}$$

where

$$\mathcal{L}(\bullet) = [1 - (e_0 a)^2 \nabla^2](\bullet) \tag{51}$$

and ∇^2 is the Laplacian.

- Using this equation the nonlocal constitutive stress-strain relation can be simplified as

$$(1 - \alpha^2 l^2 \nabla^2)\sigma_{ij} = t_{ij} \tag{52}$$

One can use this relationship and derive the equation of motion using conventional variational principle. In the next subsections we consider the dynamics of nonlocal road, beam and plate using this approach.

Nonlocal continuum mechanics

Nonlocal Parameters	Magnitudes	Researchers
a	0.142 nm	(Sudak, 2003)
e_0	0.39	(Eringen, 1983)
	0.288	(Wang and Hu, 2005)
	0-19	(Duan et al., 2007)
$e_0 a$	0.7 nm	(Wang et al, 2008)
	0-2 nm	(Duan and Wang, 2007)
	<2.1 nm	(Wang, 2005)
$e_0 a/l$	0-0.8	(Lu et al., 2006)

Values of different nonlocal parameters used in literature.

Our recent book

Our recent book has more detailed discussions on the nonlocal theory:

- Karličić, D. Murmu, T., Adhikari, S. and McCarthy, M., **Non-local Structural Mechanics**, Wiley-ISTE, 2015 (Hardback 354 pp., ISBN: 1848215223).

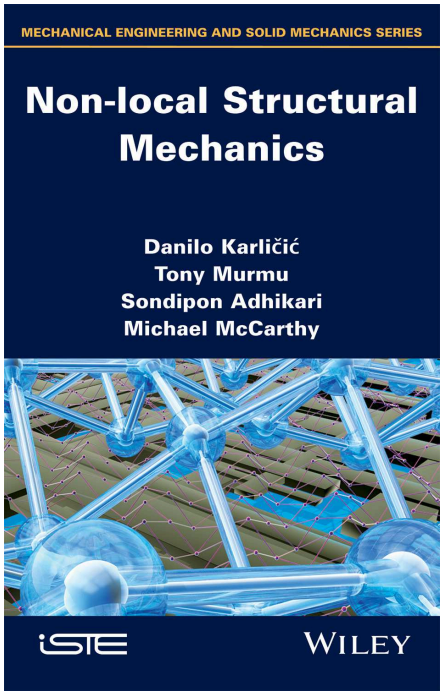

Nonlocal Resonance Frequency of CNT with Attached Biomolecule

- We consider the frequency of carbon nanotubes (CNT) with attached mass, for example, deoxythymidine molecule

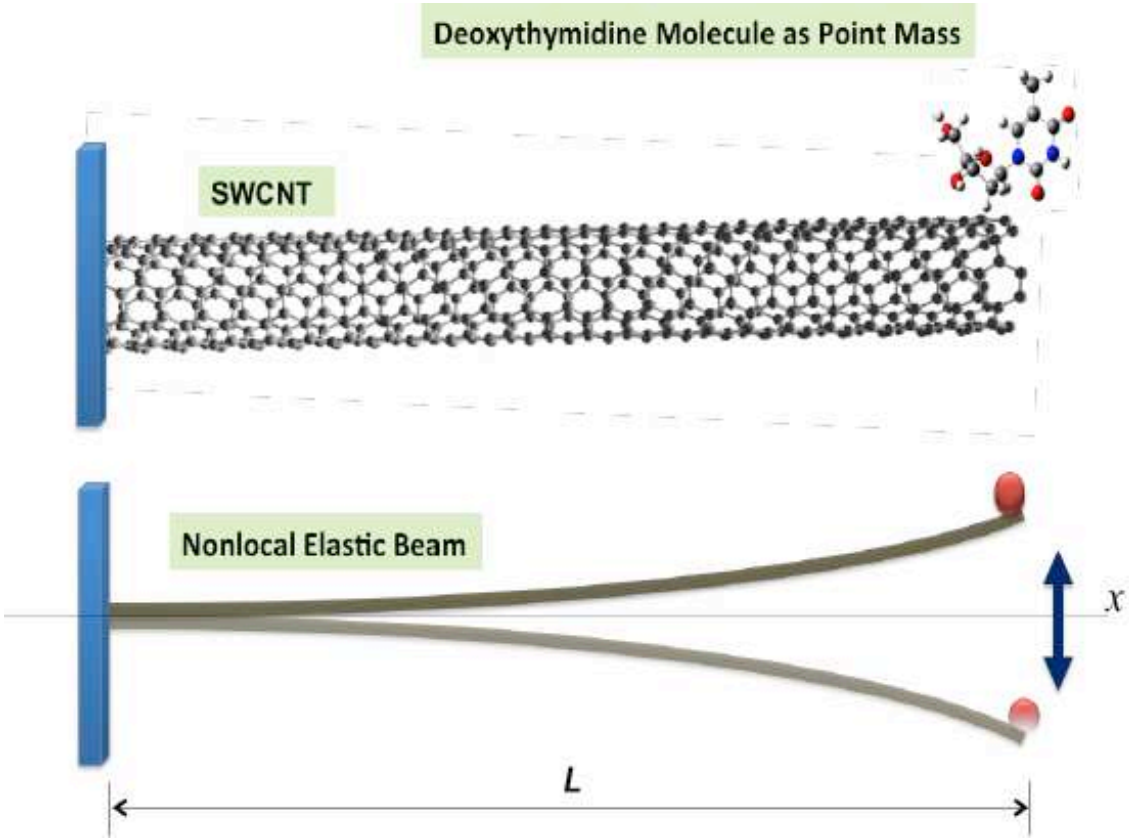

Nonlocal Resonance Frequency of CNT with Attached biomolecule

- For the bending vibration of a nonlocal damped beam, the equation of motion of free vibration can be expressed by

$$EI\frac{\partial^4 V(x,t)}{\partial x^4} + m\left(1-(e_0 a)^2\frac{\partial^2}{\partial x^2}\right)\left\{\frac{\partial^2 V(x,t)}{\partial t^2}\right\} = 0 \tag{53}$$

- In the fundamental mode of vibration, the natural frequency of a nonlocal SWCNT oscillator can be expressed as

$$f_n = \frac{1}{2\pi}\sqrt{\frac{k_{eq}}{m_{eq}}} \tag{54}$$

Here k_{eq} and m_{eq} are respectively equivalent stiffness and mass of SWCNT in the first mode of vibration.

Nonlocal resonance frequency with attached point biomolecule

- Following the energy approach, the natural frequency can be expressed as

$$f_n = \frac{1}{2\pi}\sqrt{\frac{k_{eq}}{m_{eq}}} = \frac{\beta}{2\pi}\frac{c_k}{\sqrt{1 + c_{nl}\theta^2 + c_m\Delta M}} \tag{55}$$

where

$$\beta = \sqrt{\frac{EI}{\rho A L^4}}, \theta = \frac{e_0 a}{L} \quad \text{and} \quad \Delta M = \frac{M}{\rho A L} \tag{56}$$

- The stiffness, mass and nonlocal calibration constants are

$$c_k = \sqrt{\frac{140}{11}}, c_m = \frac{140}{33} \quad \text{and} \quad c_{nl} = \frac{56}{11} \tag{57}$$

Equation (55), together with the calibration constants gives an explicit relationship between the change in the mass and frequency.

Nonlocal resonance frequency with attached distributed biomolecules

- We consider the frequency of carbon nanotubes (CNT) with attached distributed mass, for example, a collections of deoxythymidine molecules

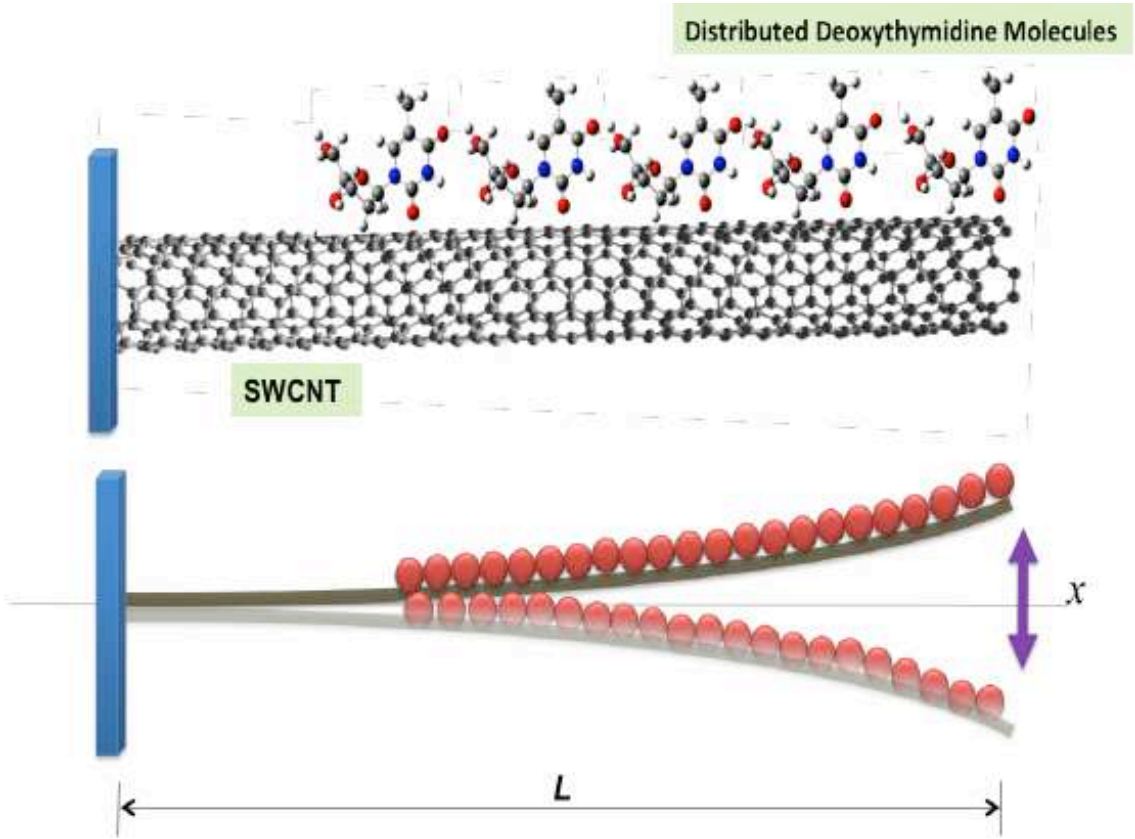

Nonlocal resonance frequency with attached distributed biomolecules

- Following the energy approach, the natural frequency can be expressed as

$$f_n = \frac{1}{2\pi}\sqrt{\frac{k_{eq}}{m_{eq}}} = \frac{\beta}{2\pi}\frac{c_k}{\sqrt{1 + c_{nl}\theta^2 + c_m(\gamma)\Delta M}} \tag{58}$$

where

$$\beta = \sqrt{\frac{EI}{\rho A L^4}}, \theta = \frac{e_0 a}{L}, \Delta M = \frac{M}{\rho A L}, c_k = \sqrt{\frac{140}{11}} \quad \text{and} \quad c_{nl} = \frac{56}{11} \tag{59}$$

- The length-dependent mass calibration constant is

$$c_m(\gamma) = \frac{140 - 210\gamma + 105\gamma^2 + 35\gamma^3 - 42\gamma^4 + 5\gamma^6}{33} \tag{60}$$

Equation (58), together with the calibration constants gives an explicit relationship between the change in the mass and frequency.

Nonlocal sensor equations

- The resonant frequency of a SWCNT with no added mass is obtained by substituting $\Delta M = 0$ in Eq. (58) as

$$f_{0_n} = \frac{1}{2\pi} c_k \beta \tag{61}$$

- Combining equations (58) and (61) one obtains the relationship between the resonant frequencies as

$$f_n = \frac{f_{0_n}}{\sqrt{1 + c_{nl}\theta^2 + c_m(\gamma)\Delta M}} \tag{62}$$

- The frequency-shift can be expressed using Eq. (62) as

$$\Delta f = f_{0_n} - f_n = f_{0_n} - \frac{f_{0_n}}{\sqrt{1 + c_{nl}\theta^2 + c_m(\gamma)\Delta M}} \tag{63}$$

- From this we obtain

$$\frac{\Delta f}{f_{0_n}} = 1 - \frac{1}{\sqrt{1 + c_{nl}\theta^2 + c_m(\gamma)\Delta M}} \tag{64}$$

Nonlocal sensor equations

- Rearranging gives the expression

Relative mass detection

$$\Delta M = \frac{1}{c_m(\gamma)\left(1-\frac{\Delta f}{f_{0_n}}\right)^2} - \frac{c_{nl}}{c_m(\gamma)}\theta^2 - \frac{1}{c_m(\gamma)} \tag{65}$$

- This equation completely relates the change in mass with the frequency-shift using the mass calibration constant. The actual value of the added mass can be obtained from (65) as

Absolute mass detection

$$M = \frac{\rho AL}{c_m(\gamma)}\frac{\left(c_k^2\beta^2\right)}{\left(c_k\beta - 2\pi\Delta f\right)^2} - \frac{c_{nl}}{c_m(\gamma)}\theta^2\rho AL - \frac{\rho AL}{c_m(\gamma)} \tag{66}$$

This is the general equation which completely relates the added mass and the frequency shift using the calibration constants.

Zigzag (5,0) SWCNT of length 8.52 nm with added DeOxy Thymidine (a nucleotide that is found in DNA)

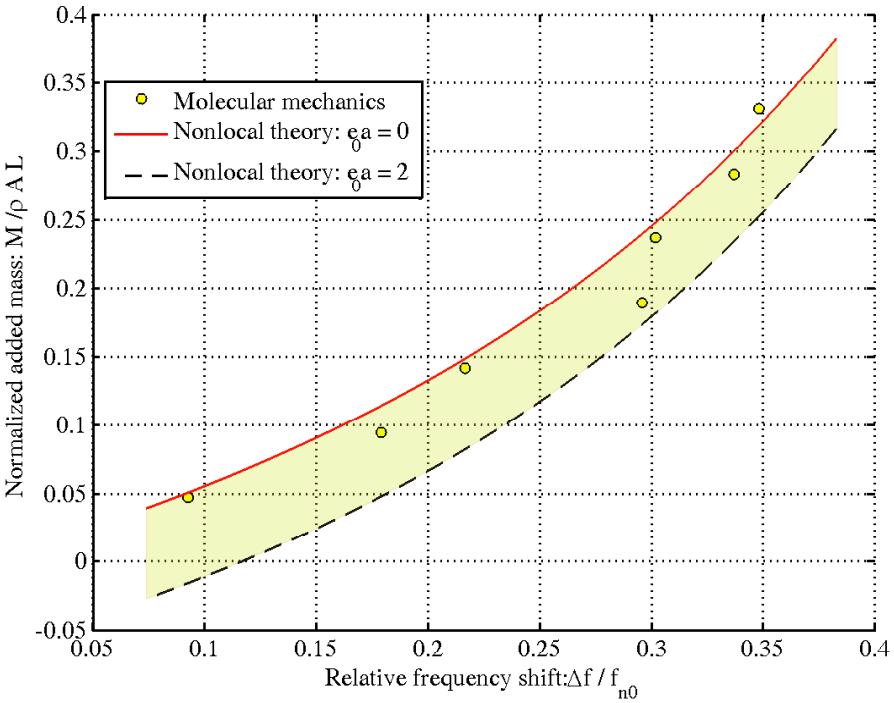

(a) Point mass on a cantilevered CNT.

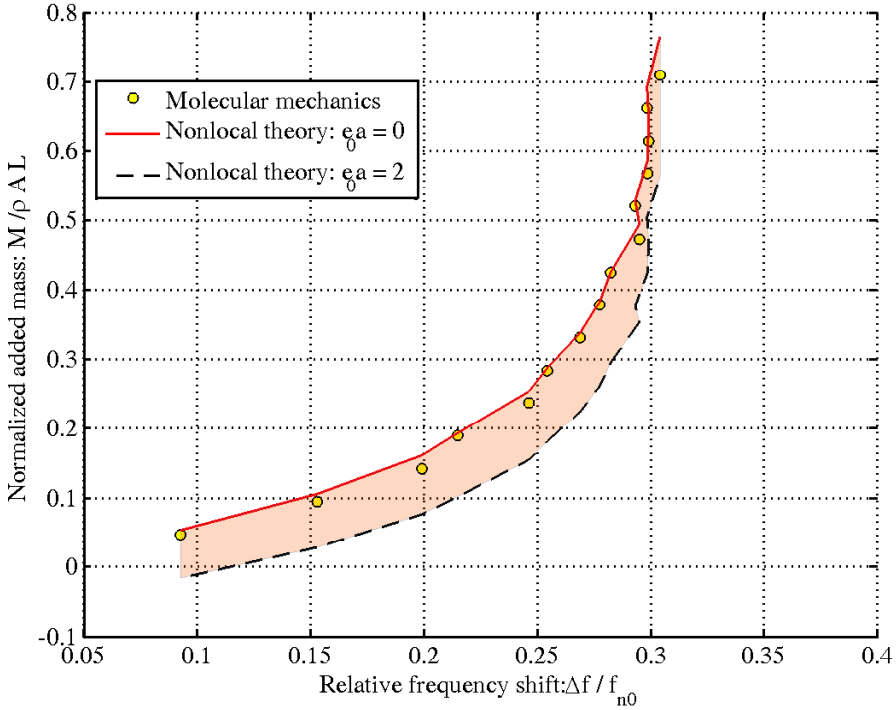

(b) Distributed mass on a cantilevered CNT. The length of the mass varies between $0.05L$ to $0.72L$ from the edge of the CNT.

Figure: Normalized mass vs. relative frequency shift for the SWCNT with point mass. The band covers the complete range of nonlocal the parameter $0 \leq e_2 \leq 2$nm. It can be seen that the molecular mechanics simulation results reasonably fall within this band (except at $\Delta f / f_{n0}$=0.35).

Results for optimal values of the nonlocal parameter

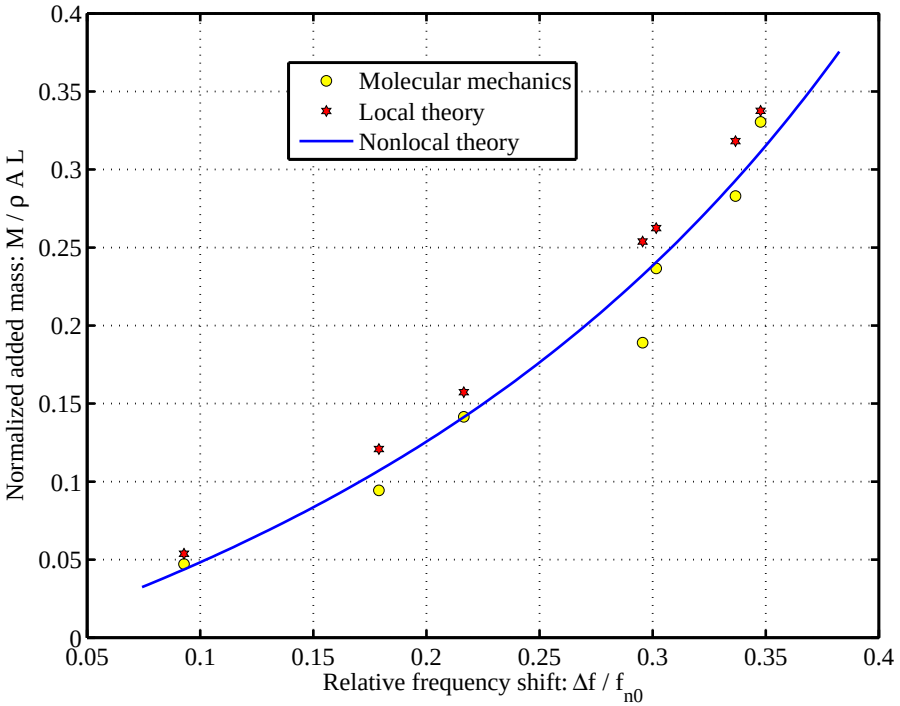

(a) Point mass on a cantilevered CNT: $e_0 a =$ 0.65nm.

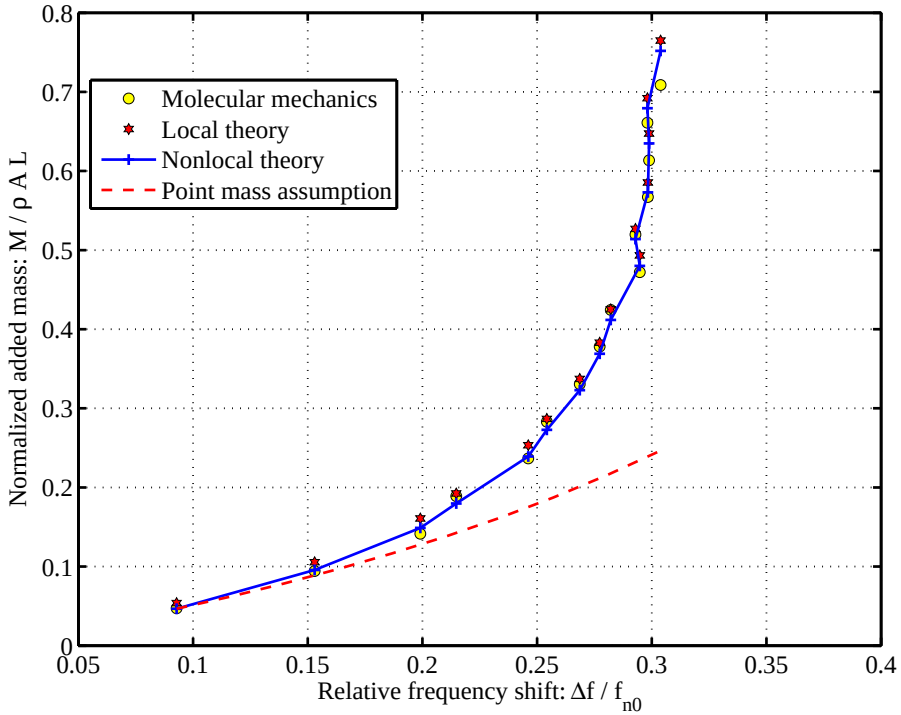

(b) Distributed mass on a cantilevered CNT. $e_0 a = 0.5$nm.

Figure: Normalized mass vs. relative frequency shift for the SWCNT with point mass with optimal values of the nonlocal parameter $e_0 a$.

Error in mass detection: point mass

Percentage error in the mass detection using cantilevered CNT based biosensors for single biomolecule. The errors are shown for both local and nonlocal elastic theories (with optimised nonlocal parameter $e_0 a = 0.65$ nm).

Relative frequency shift	Percentage error	
	Local elasticity	Nonlocal elasticity
0.0929	13.9879	7.3226
0.179	28.1027	13.3841
0.2165	11.1765	0.1131
0.2956	34.2823	22.9147
0.3016	10.9296	1.6392
0.3367	12.4422	3.5486
0.3477	2.1427	5.807

Error in mass detection: distributed mass

Percentage errors in the mass detection using cantilevered CNT based biosensor for distributed added biomolecules. The errors are shown for both local and nonlocal elastic theories (with optimised nonlocal parameter $e_0 a = 0.5$ nm).

Relative frequency shift	Normalized length	Percentage error	
		Local elasticity	Nonlocal elasticity
0.0929	0	13.9879	1.2813
0.153	0.05	11.8626	1.4132
0.1991	0.1	13.7038	5.171
0.2148	0.15	1.7865	4.9412
0.2462	0.2	7.0172	1.0914
0.2542	0.25	1.3278	3.6149
0.2687	0.3	1.9943	2.2774
0.2773	0.35	1.2631	2.4081
0.2821	0.4	0.1653	3.0046
0.2948	0.45	4.515	1.7056
0.2929	0.5	1.3776	1.0761
0.2983	0.55	3.2275	1.0155
0.2989	0.6167	5.524	3.4922
0.2981	0.6667	4.6735	2.7585
0.3039	0.7167	7.9455	6.0986

Single-layer graphene sheet (SLGS) based sensors

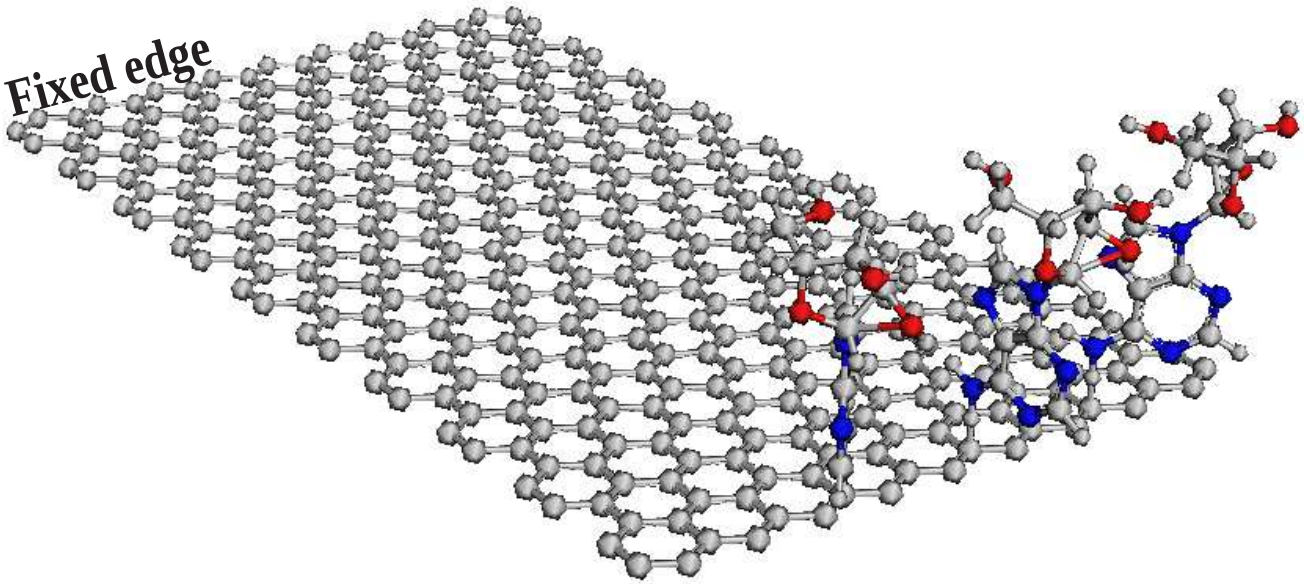

Cantilevered Single-layer graphene sheet (SLGS) with adenosine molecules

Resonant frequencies of SLGS with attached mass

- We model SLGS dynamics as a thin plate in transverse vibration:

$$D\left(\frac{\partial^4 u}{\partial x^4}+2\frac{\partial^2 u}{\partial x^2}\frac{\partial^2 u}{\partial y^2}+\frac{\partial^4 u}{\partial y^4}\right)+\rho\frac{\partial^2 u}{\partial t^2}=0, \tag{67}$$
$$0\leq x\leq a;\ 0\leq y\leq b.$$

- Here $u\equiv u(x,y,t)$ is the transverse deflection, x, y are coordinates, t is the time, ρ is the mass density per area and the bending rigidity is defined by

$$D=\frac{Eh^3}{12(1-\nu^2)} \tag{68}$$

- E is the Young's modulus, h is the thickness and ν is the Poisson's ratio. We consider rectangular graphene sheets with cantilevered (clamped at one edge) boundary condition.

Resonant frequencies of SLGS

- The vibration mode-shape for the first mode of vibration of the planar SLGS is given by

$$w(x, y) = 1 - \cos(\pi x/2a) \tag{69}$$

- The natural frequency of the system can be alternatively obtained using the energy principle. Assuming the harmonic motion, the kinetic energy of the vibrating plate can be expressed by

$$T = \omega^2 \int_A w^2(x, y)\rho \mathrm{d}A \tag{70}$$

- Here ω denotes the frequency of oscillation and A denotes the area of the plate. Using the expression of $w(x, y)$ in Eq. (69) we have

$$\begin{aligned} T &= \frac{1}{2}\omega^2\rho \int_0^a \int_0^b (1 - \cos(\pi x/2a))^2 \,\mathrm{d}x\,\mathrm{d}y \\ &= \frac{1}{2}\omega^2(ab\rho)\frac{3\pi - 8}{2\pi} \end{aligned} \tag{71}$$

Resonant frequencies of SLGS

- The potential energy can be obtained as

$$U = \frac{D}{2}\int_A \left\{ \left(\frac{\partial^2 w}{\partial x^2} + \frac{\partial^2 w}{\partial y^2} \right)^2 - 2(1-\nu)\left[\frac{\partial^2 w}{\partial x^2}\frac{\partial^2 w}{\partial y^2} - \left(\frac{d^2 w}{dx^2} y \right)^2 \right] \right\} \mathrm{d}A \tag{72}$$

- Using the expression of $w(x, y)$ in (69) we have

$$U = \frac{D}{2}\rho \int_0^a \int_0^b \left(\frac{\partial^2 w}{\partial x^2} \right)^2 \mathrm{d}x\,\mathrm{d}y = \frac{1}{2}\frac{\pi^4 D}{a^3} b(1/32) \tag{73}$$

- Considering the energy balance, that is $T_{\max} = U_{\max}$, from Eqs. (83) and (73) the resonance frequency can be obtained as

$$\omega_0^2 = \left(\frac{\pi^4 D}{a^4 \rho} \right) \frac{1/32}{(3\pi - 8)/2\pi} \tag{74}$$

Resonant frequencies of SLGS with attached mass

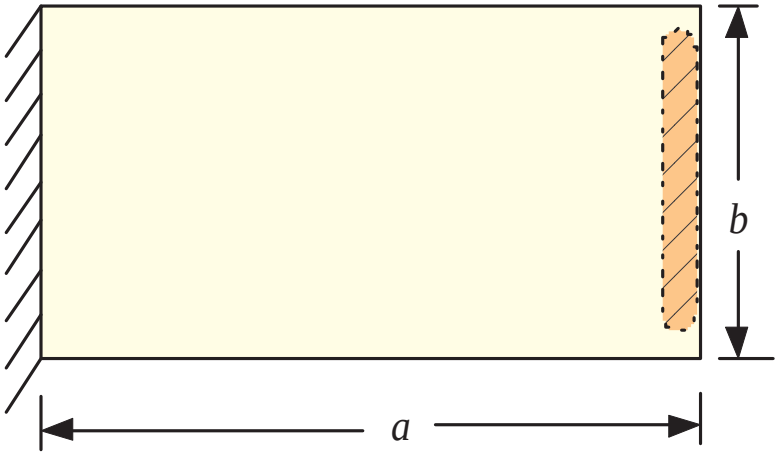

(a) Masses at the cantilever tip in a line

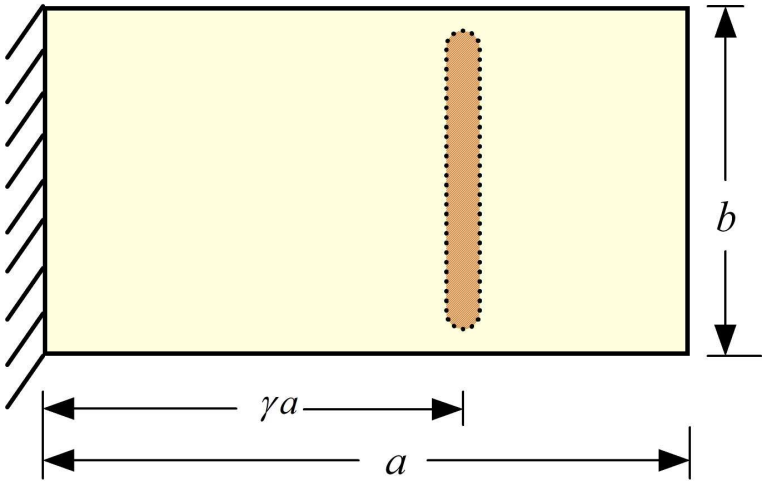

(b) Masses in a line along the width

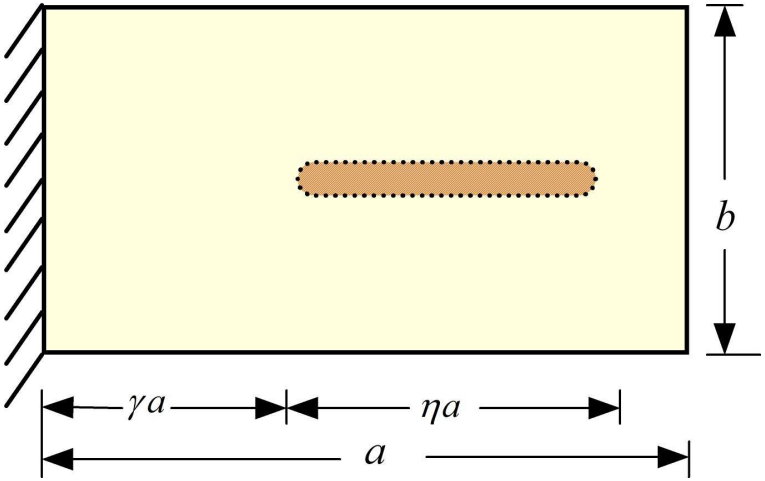

(c) Masses in a line along the length

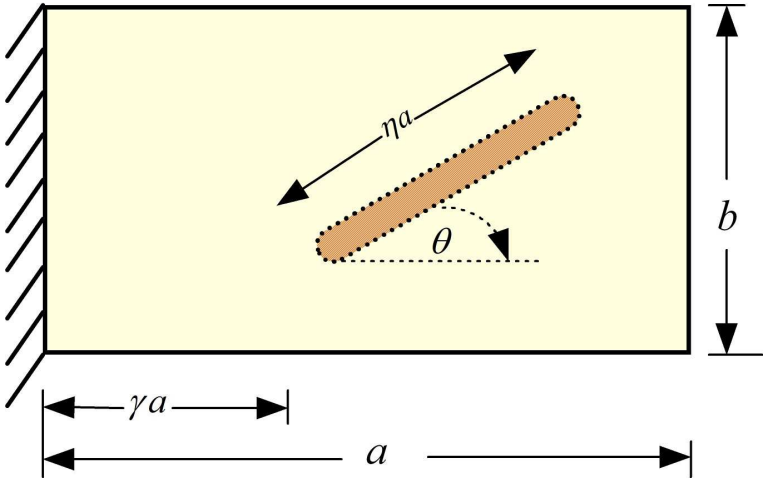

(d) Masses in a line with an arbitrary angle

Resonant frequencies of SLGS with attached mass

- Using the energy approach, the resonance frequency can be expressed in a general form as

$$\omega^2_{a,b,c,d} = \frac{\frac{1}{2}\frac{\pi^4 D}{a^3} b(1/32)}{\frac{1}{2}\left\{ab\rho\frac{3\pi-8}{2\pi} + \alpha_{a,b,c,d}M\right\}} = \left(\frac{\pi^4 D}{a^4\rho}\right)\frac{1/32}{(3\pi-8)/2\pi + \mu\alpha_{b,c,d}} \tag{75}$$

- Here the ratio of the added mass

$$\mu = \frac{M}{M_g} \tag{76}$$

- $\alpha_{a,b,c,d}$ are factors which depend on the mass distribution:.

$$\alpha_a = 1, \quad \alpha_b = (1-\cos(\pi\gamma/2))^2 \tag{77}$$

$$\alpha_c = \frac{3\pi\eta + [\sin((\gamma+\eta)\pi) - \sin(\gamma\pi)] - 8[\sin((\gamma+\eta)\pi/2) - \sin(\gamma\pi/2)]}{2\pi\eta} \tag{78}$$

$$\alpha_d = \frac{3\pi\eta\cos(\theta) + [\sin((\gamma+\eta\cos(\theta))\pi) - \sin(\gamma\pi)] - 8[\sin((\gamma+\eta\cos(\theta))\pi/2) - \sin(\gamma\pi/2)]}{2\pi\eta\cos(\theta)} \tag{79}$$

Sensor equation

- The relative added mass of the bio-fragment can be obtained from the frequency shift as

Relative mass detection for 2D sensors

$$\mu = \frac{1}{c_n\left(1-\frac{\Delta f}{f_0}\right)^2} - \frac{1}{c_n} \tag{80}$$

Mass arrangement	Calibration constant c_n
Case (a): Masses are at the cantilever tip in a line	$2\pi/(3\pi-8)$
Case (b): Masses are in a line along the width	$2\pi(1-\cos(\pi\gamma/2))^2/(3\pi-8)$
Case (c): Masses are in a line along the length	$(3\pi\eta+[\sin((\gamma+\eta)\pi)-\sin(\gamma\pi)]-8[\sin((\gamma+\eta)\pi/2)-\sin(\gamma\pi/2)])/\eta(3\pi-8)$
Case (d): Masses are in a line with an arbitrary angle θ	$(3\pi\eta\cos(\theta)+[\sin((\gamma+\eta\cos(\theta))\pi)-\sin(\gamma\pi)]-8[\sin((\gamma+\eta\cos(\theta))\pi/2)-\sin(\gamma\pi/2)])/\eta\cos(\theta)(3\pi-8)$

Validation with MM simulation (UFF): Case a

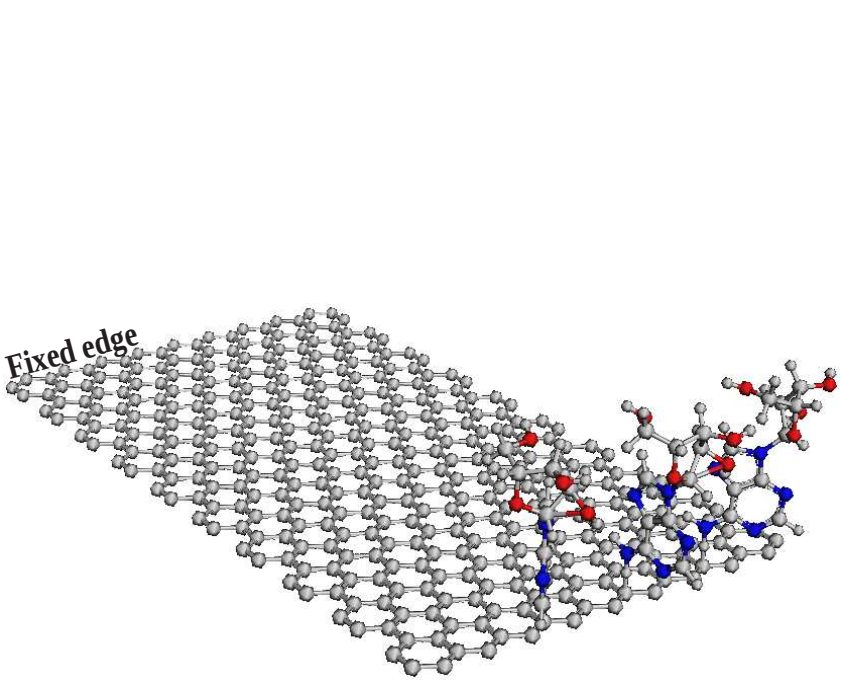

(a) SLGS with adenosine molecules at the cantilever tip in a line

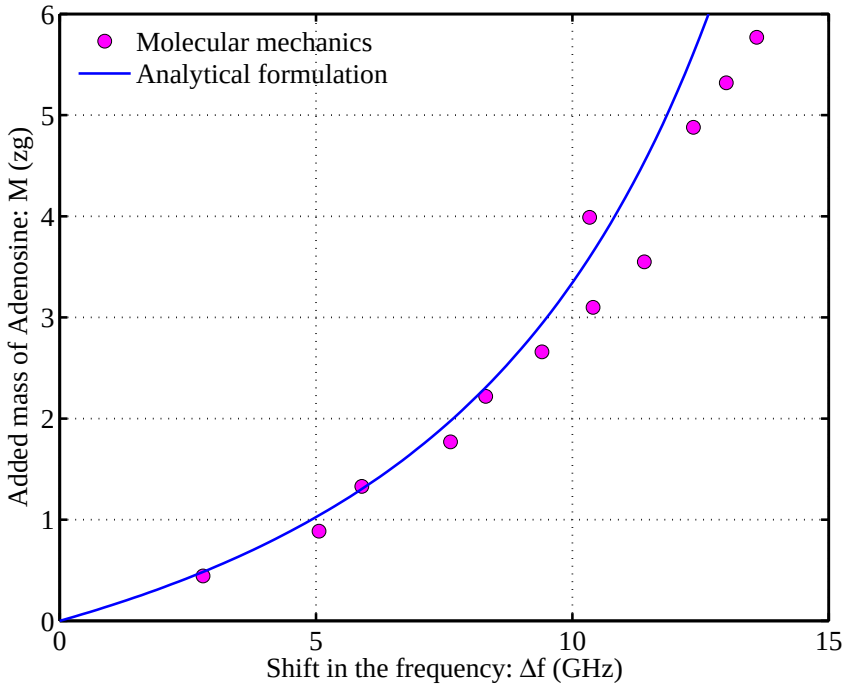

(b) Identified mass from the frequency shift

Figure: Identified attached masses from the frequency-shift of a cantilevered SLGS resonator for case (a). The SLGS mass is 7.57zg and the mass of each adenosine molecule is 0.44zg. The proposed approach is validated using data from the molecular mechanics simulations. Up to 12 adenosine molecules are attached to the graphene sheet.

Validation with MM simulation: Case b

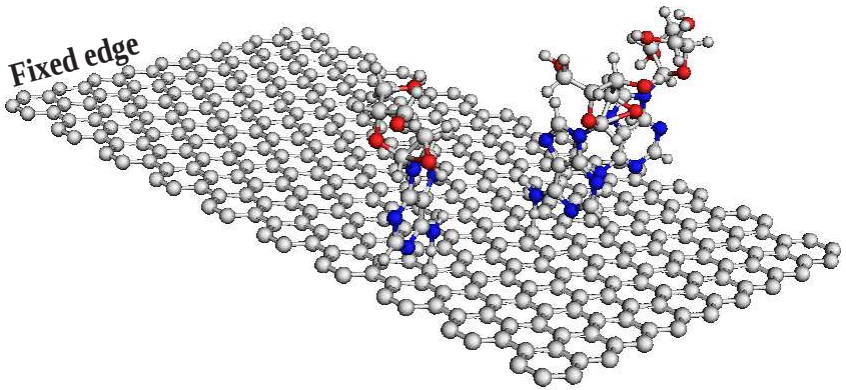

(a) SLGS with adenosine molecules in a line along the width

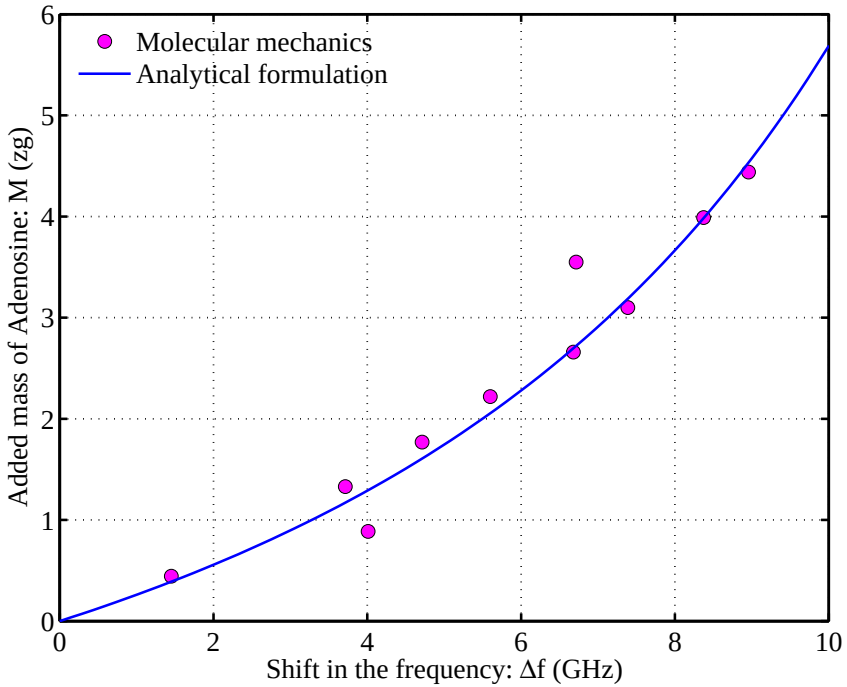

(b) Identified mass from the frequency shift, $\gamma = 0.85$

Figure: Identified attached masses from the frequency-shift of a cantilevered SLGS resonator for case (b). The proposed approach is validated using data from the molecular mechanics simulations. Up to 10 adenosine molecules are attached to the graphene sheet.

Validation with MM simulation: Case d

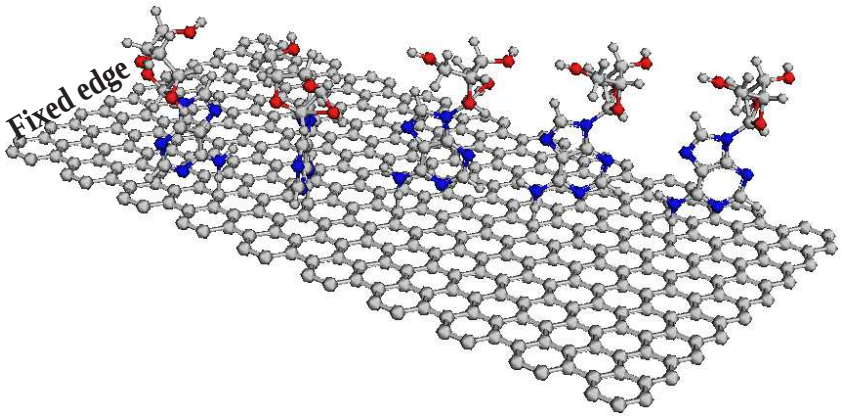

(a) SLGS with adenosine molecules in a line with an arbitrary angle

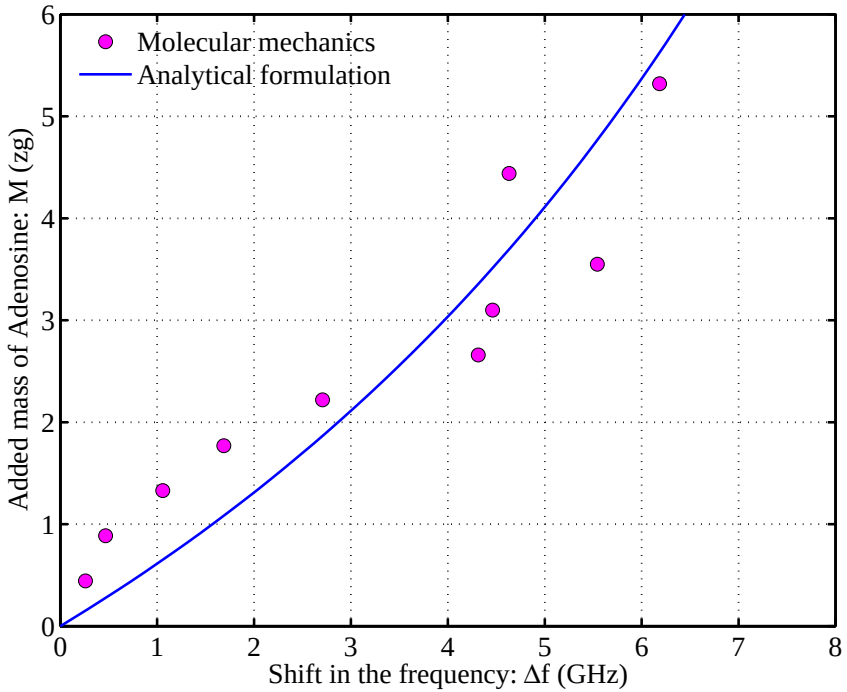

(b) Identified mass from the frequency shift, $\gamma = 0.25$, $\eta = 0.7$ and $\theta = \pi/6$

Figure: Identified attached masses from the frequency-shift of a cantilevered SLGS resonator for case (d). The proposed approach is validated using data from the molecular mechanics simulations. Up to 10 adenosine molecules are attached to the graphene sheet.

Nonlocal plate theory for SLGS

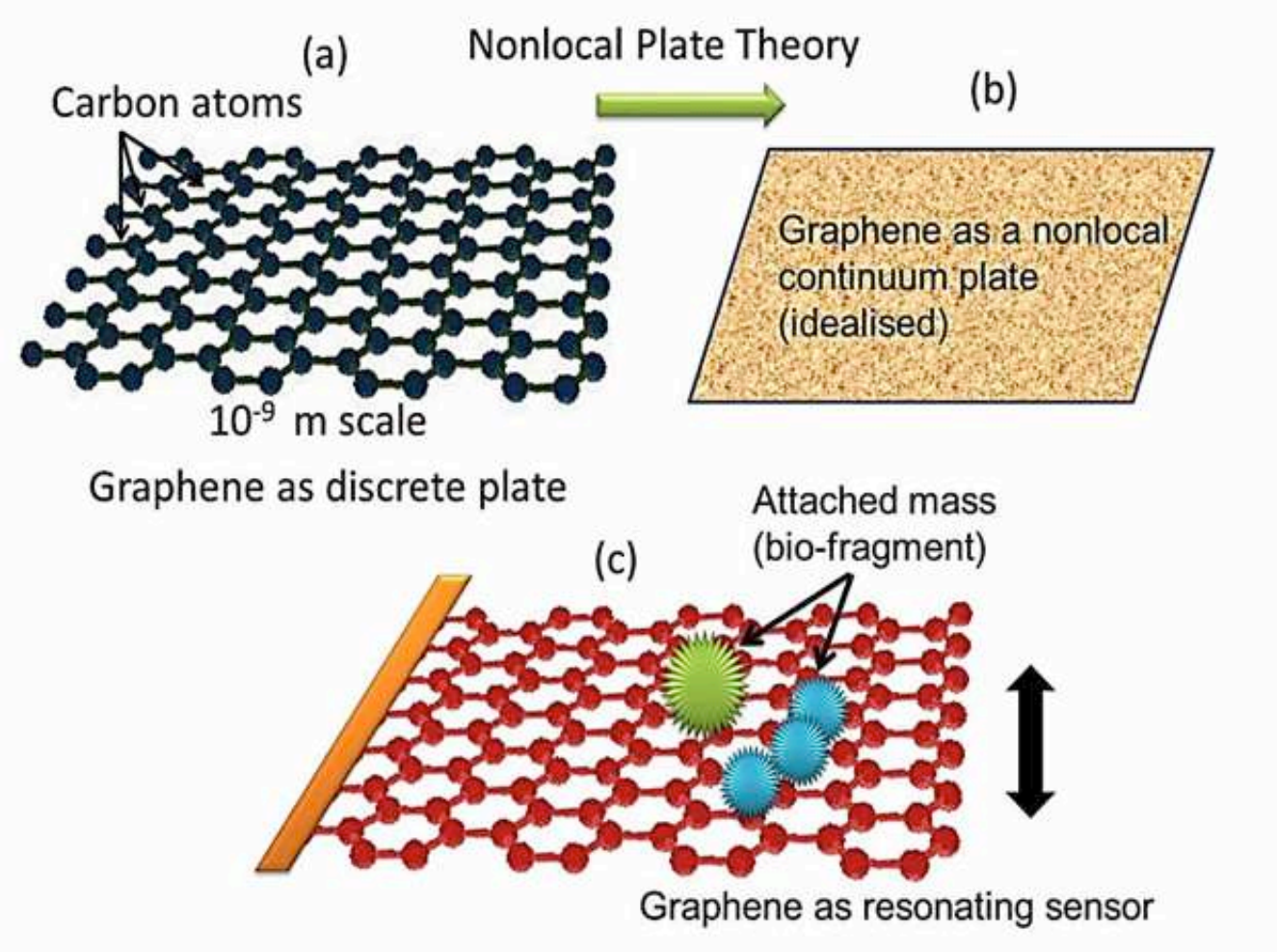

(a) Schematic diagram of single-layer graphene sheets, (b) Nonlocal continuum plate as a model for graphene sheets, (c) Resonating graphene sheets sensors with attached bio fragment molecules such as adenosine.

Nonlocal plate theory for SLGS

- We model SLGS dynamics as a thin nonlocal plate in transverse vibration

$$D\nabla^4 u + m\left(1 - (e_0 a)^2\nabla^2\right)\left\{\frac{\partial^2 u}{\partial t^2}\right\}, \tag{81}$$
$$0 \leq x \leq c;\ 0 \leq y \leq b.$$

- Here $u \equiv u(x, y, t)$ is the transverse deflection, $\nabla^2 = \left(\frac{\partial^2}{\partial x^2} + \frac{\partial^2}{\partial x^2}\right)$ is the differential operator, x, y are coordinates, t is the time, ρ is the mass density per area and the bending rigidity is defined by

$$D = \frac{Eh^3}{12(1-\nu^2)} \tag{82}$$

- Introducing the non dimensional length scale parameter

$$\mu = \frac{e_0 a}{c} \tag{83}$$

the resonance frequency can be obtained as

$$\omega_0^2 = \left(\frac{\pi^4 D}{c^4 \rho}\right)\frac{1/32}{(3\pi - 8)/2\pi + \mu^2\pi^2/8} \tag{84}$$

Nonlocal SLGS with attached masses

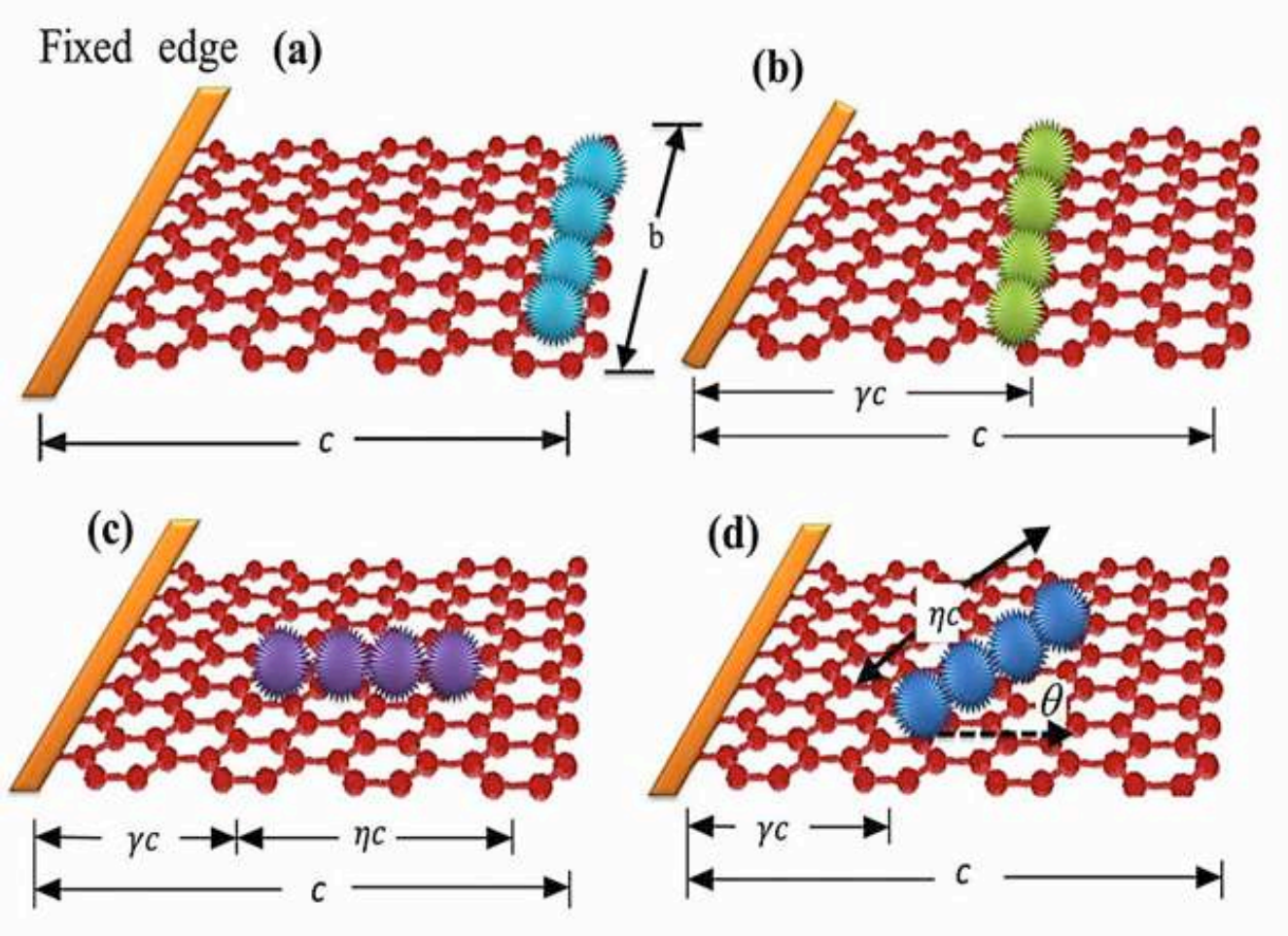

(a) Masses at the cantilever tip in a line (b) masses in a line along the width, (c) masses in a line along the length, (d) masses in a line with an arbitrary angle.

Nonlocal resonant frequencies of SLGS with attached mass

- Using the energy approach, the resonance frequency can be expressed in a general form as

$$\omega^2_{a,b,c,d} = \frac{\frac{1}{2}\frac{\pi^4 D}{c^3} b(1/32)}{\frac{1}{2}\left\{cb\rho\left(\frac{3\pi-8}{2\pi} + \frac{\mu^2\pi^2}{8}\right) + \alpha_{a,b,c,d}M\right\}}$$
$$= \left(\frac{\pi^4 D}{c^4\rho}\right)\frac{1/32}{(3\pi-8)/2\pi + \mu^2\pi^2/8 + \beta\alpha_{b,c,d}} \tag{85}$$

- Here the ratio of the added mass

$$\beta = \frac{M}{M_g} \tag{86}$$

and $\alpha_{b,c,d}$ are factors which depend on the mass distribution as defined before.

Free vibration response of nonlocal SLGS with attached masses

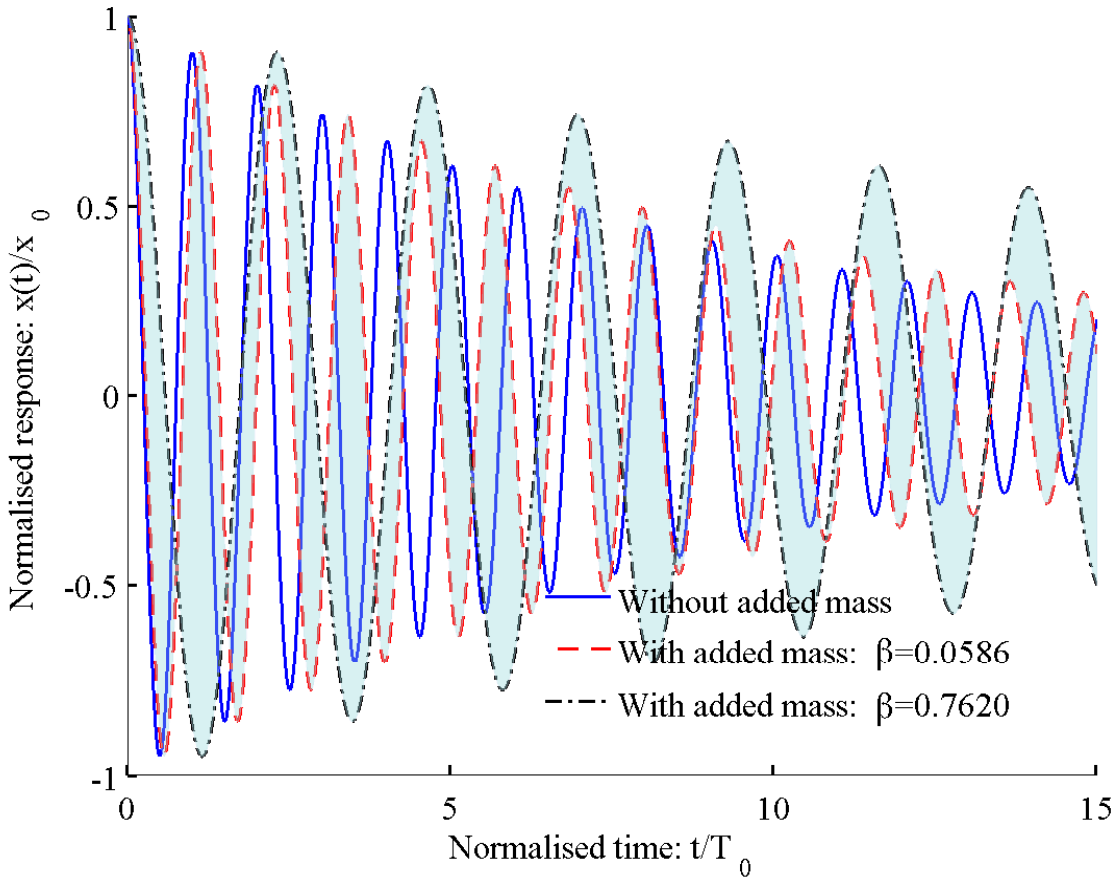

Free vibration response at the tip of the graphene sheet due to the unit initial displacement obtained from molecular mechanics simulation. Here T_0 is the time period of oscillation without any added mass. The shaded area represents the motion of all the mass loading cases considered for case (a).

Validation with MM simulation (UFF): Case a

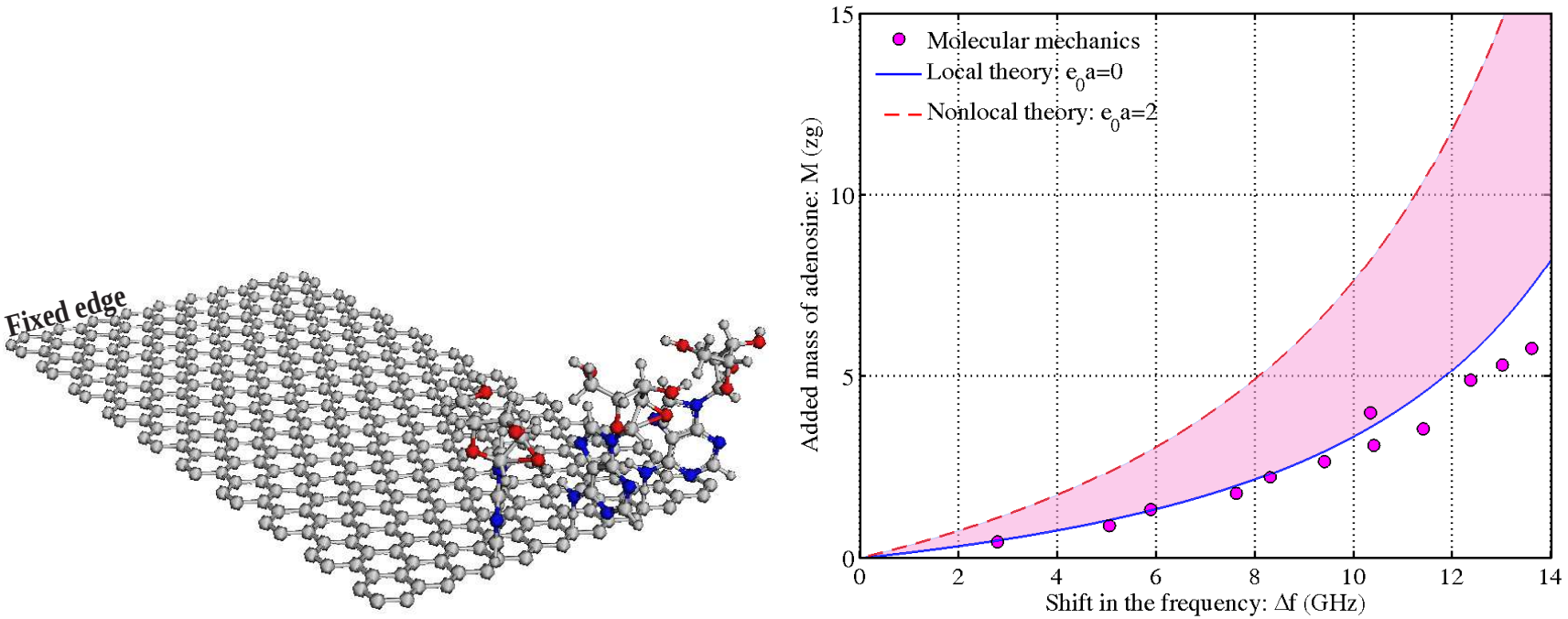

(a) SLGS with adenosine molecules at the cantilever tip in a line

(b) Identified mass from the frequency shift

Figure: Identified attached masses from the frequency-shift of a cantilevered SLGS resonator for case (a). The SLGS mass is 7.57zg and the mass of each adenosine molecule is 0.44zg. The proposed approach is validated using data from the molecular mechanics simulations. Up to 12 adenosine molecules are attached to the graphene sheet.

Validation with MM simulation: Case b

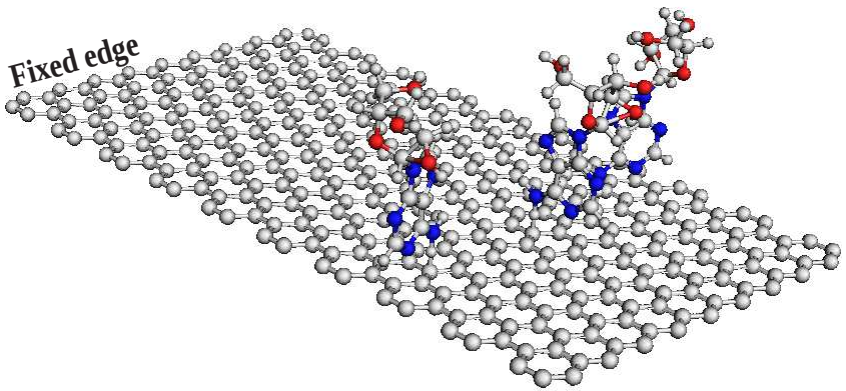

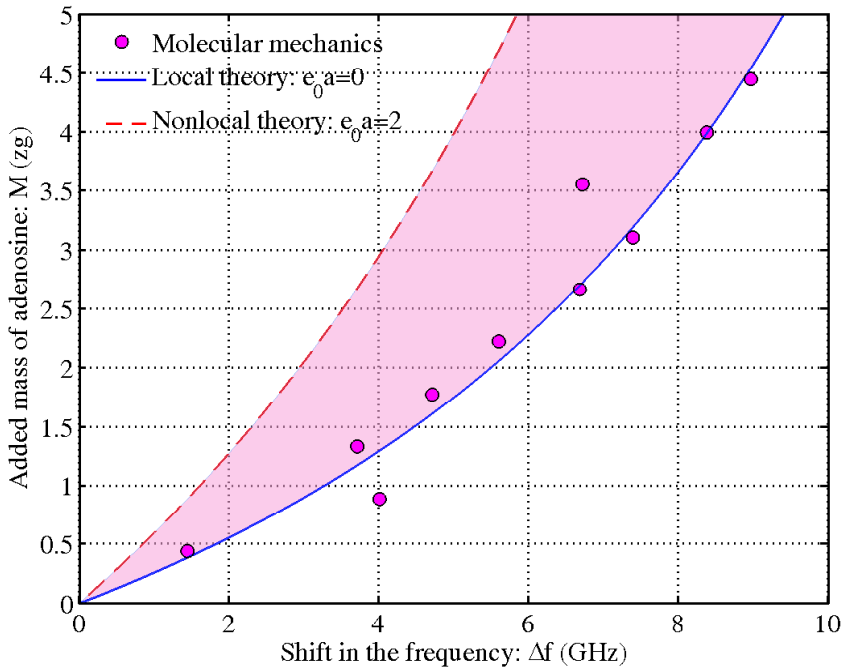

(a) SLGS with adenosine molecules in a line along the width

(b) Identified mass from the frequency shift, $\gamma = 0.85$

Figure: Identified attached masses from the frequency-shift of a cantilevered SLGS resonator for case (b). The proposed approach is validated using data from the molecular mechanics simulations. Up to 10 adenosine molecules are attached to the graphene sheet.

Validation with MM simulation: Case d

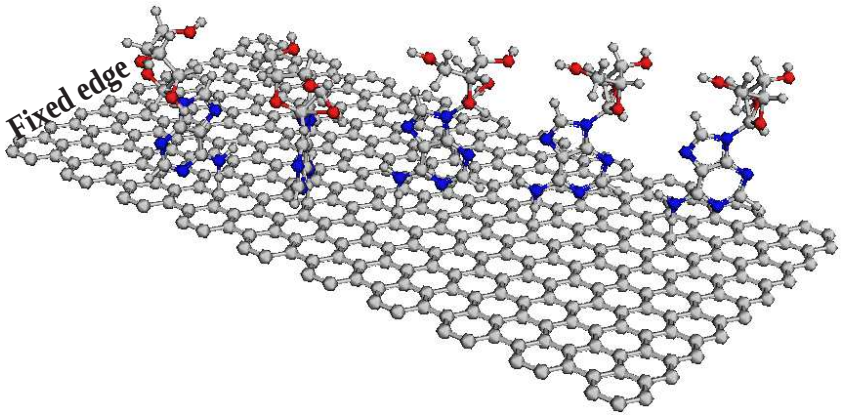

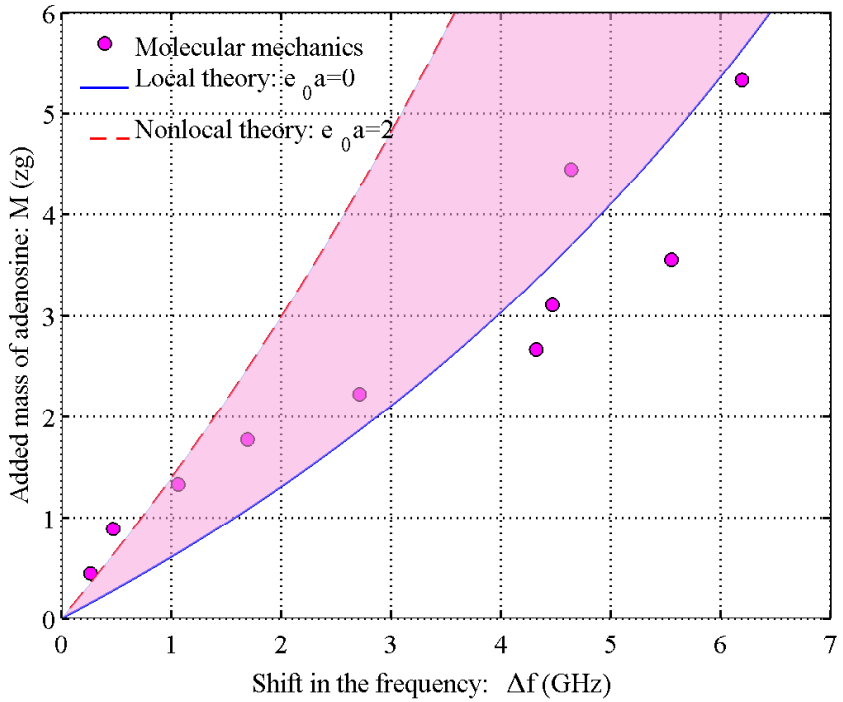

(a) SLGS with adenosine molecules in a line with an arbitrary angle

(b) Identified mass from the frequency shift, $\gamma = 0.25$, $\eta = 0.7$ and $\theta = \pi/6$

Figure: Identified attached masses from the frequency-shift of a cantilevered SLGS resonator for case (d). The proposed approach is validated using data from the molecular mechanics simulations. Up to 10 adenosine molecules are attached to the graphene sheet.

Conclusions

- Principles of fundamental mechanics and dynamics can have unprecedented role in the development of nano-mechanical bio sensors. Nano-sensor market is predicted to be over 20 Billion$ by 2020.
- Mass sensing is an inverse problem - NOT a conventional “forward problem”.
- Due to the need for “instant calculation”, physically insightful simplified (but approximate) approach is more suitable compared to very detailed (but accurate) molecular dynamic simulations.
- Energy based simplified dynamic approach turned out to sufficient to identify mass of the attached bio-objects from “measured” frequency-shifts in nano-scale sensors.
- Closed-form sensor equations have been derived and independently validated using molecular mechanics simulations. Calibration constants necessary for this approach have been given explicitly for point mass as well as distributed masses.
- Nonlocal model with optimally selected length-scale parameter improves the mass detection capability for nano-sensors.

[1] Chowdhury, R., Adhikari, S., and Mitchell, J., "Vibrating carbon nanotube based bio-sensors," *Physica E: Low-Dimensional Systems and Nanostructures*, Vol. 42, No. 2, December 2009, pp. 104–109.

[2] Adhikari, S. and Chowdhury, R., "The calibration of carbon nanotube based bio-nano sensors," *Journal of Applied Physics*, Vol. 107, No. 12, 2010, pp. 124322:1–8.

[3] Chowdhury, R., Adhikari, S., Rees, P., Scarpa, F., and Wilks, S. P., "Graphene based bio-sensor using transport properties," *Physical Review B*, Vol. 83, No. 4, 2011, pp. 045401:1–8.

[4] Chowdhury, R. and Adhikari, S., "Boron nitride nanotubes as zeptogram-scale bio-nano sensors: Theoretical investigations," *IEEE Transactions on Nanotechnology*, Vol. 10, No. 4, 2011, pp. 659–667.

[5] Murmu, T. and Adhikari, S., "Nonlocal frequency analysis of nanoscale biosensors," *Sensors & Actuators: A. Physical*, Vol. 173, No. 1, 2012, pp. 41–48.

[6] Adhikari, S. and Chowdhury, R., "Zeptogram sensing from gigahertz vibration: Graphene based nanosensor," *Physica E: Low-dimensional Systems and Nanostructures*, Vol. 44, No. 7-8, 2012, pp. 1528–1534.

[7] Adhikari, S. and Murmu, T., "Nonlocal mass nanosensors based on vibrating monolayer graphene sheets," *Sensors & Actuators: B. Chemical*, Vol. 188, No. 11, 2013, pp. 1319–1327.

[8] Kam, K., Scarpa, F., Adhikari, S., and Chowdhury, R., "Graphene nanofilm as pressure and force sensor: a mechanical analysis," *Physica Status Solidi B*, Vol. 250, No. 10, 2013, pp. 2085–2089.

[9] Sheady, Z. and Adhikari, S., "Cantilevered biosensors: Mass and rotary inertia identification," *Proceedings of the 11th Annual International Workshop on Nanomechanical Sensing (NMC 2014)*, Madrid, Spain, May 2014.

[10] Clarke, E. and Adhikari, S., "Two is better than one: Weakly coupled nano cantilevers show ultra-sensitivity of mass detection," *Proceedings of the 11th Annual International Workshop on Nanomechanical Sensing (NMC 2014)*, Madrid, Spain, May 2014.

[11] Karlicic, D., Kozic, P., Adhikari, S., Cajic, M., Murmu, T., and Lazarevic, M., "Nonlocal biosensor based on the damped vibration of single-layer graphene influenced by in-plane magnetic field," *International Journal of Mechanical Sciences*, Vol. 96-97, No. 6, 2015, pp. 101–109.